Norwegian University
of Life Sciences

Master's Thesis 2022 60 ECTS
Faculty of Chemistry, Biotechnology and Food Science

Assessing the potential of Norwegian fungal isolates for biodegrading low-density polyethylene (LDPE)

Jan Ola Fodnes
Biotechnology

Acknowledgment

This work was the thesis at the end of a two-year master's degree in biotechnology at the faculty of Chemistry, Biotechnology and Food (KBM) at the Norwegian University of Life Science (NMBU). The task was performed with the help of the Norwegian Veterinary Institute (NVI) The Imaging Center (NMBU) and Nofima AS. Laboratory work was done at all the mentioned places, but primarily at NMBU and NVI. The thesis makes up 60 ECTS and lasted the entire academic year of 2021–2022. This last year has been a highly educational where I have gained insight into new disciplines and learned several new techniques.

There are many people who deserve recognition for having contributed to this thesis. I would like to start by thanking the welcoming colleagues at the NVI for always being positive and encouraging. An extra thank you to Mykoklan for professional discussions and the introduction to the wonderous world of mycology. The assistance provided by Ellen Christensen for guidance in microscopy and morphological identification was greatly appreciated. I would like to specially thank Elin Rolén for guidance in molecular identification and for listening to me. I wish to show my appreciation to Rannei Tjåland and Else Marie Aasen for assistance in the laboratory at NMBU, and for always showing curiosity and interest.

I would like to thank Lene Cecilie Hermansen and Hilde Raanaas Kolstad at The Imaging Center (NMBU) for their patience and introduction to SEM. I would also like to thank Nils Kristian Afseth and Ulrike Böcker at Nofima for your patience with my repeated visits to your FTIR and computer lab, the ATR-FTIR results would not be as they were without you.

I wish to extend my special thanks to my supervisors Ida Skaar (NMBU / NVI) and Hege Hvattum Divon (NVI) for making the thesis possible, the impeccable guidance, trust and great freedom.

A final invaluable thank you goes to my dear Sophie Maria Pursti who has endured me throughout my education. I wish to thank you so much for the professional discussions, not so professional discussions, proofreading and revision of the thesis and for always showing up in moments of need.

Ås 15.06.2022 Jan Ola Fodnes

Abstract

The enormous amounts of plastic waste generated are a global environmental problem, as plastics are found in environments and ecosystems around the world. Mycologists have joined the collective effort in remedying this problem and have discovered plastic degrading potential in several fungal species. This study seeks to explore Norwegian environments to isolate fungi with plastic degrading capabilities. This was done by isolating and identifying 11 isolates from soil samples collected from six different locations in Norway. An additional five species that the literature have reported to have Low-Density Polyethylene (LDPE) degrading capabilities were selected from the fungal strain collection of the Norwegian Veterinary Institute (*Mykoteket*). The 16 isolates were incubated in liquid media with LDPE test objects for 30, 60 and 90 days at 20 °C to observe the fungal potential to degrade LDPE plastic. The experiment was done in two parallels, with and without glucose. After incubation the mass of LDPE test objects and freeze-dried fungal biomass were recorded, and the test objects were analyzed by SEM, ATR-FTIR. SEM imaging revealed potential evidence of biological degradation in three of the fungal isolates incubated for 90 days, as fractures and roughness was observed on the surface of the test objects. No changes in the test objects were observed by ATR-FTIR or in the freeze-dried biomass or test object weight loss, regardless of presence of glucose, isolate or incubation period. The results are however non-conclusive in relation to the fungal isolates capabilities of degrading LDPE. Based on experience gained from this pilot study, some optimizations of the study design and methods are recommended before further research on plastic degrading fungi found in Norwegian environments is performed.

Sammendrag

De enorme mengdene plastavfall som genereres er et globalt miljøproblem, ettersom plast finnes i miljøer og økosystemer rundt om i verden. Mykologer har sluttet seg til den kollektive innsatsen for å avhjelpe dette problemet og har oppdaget potensiale for nedbrytning av plast hos flere sopparter. Denne studien søker å utforske norske miljøer for å isolere muggsopp med egenskaper egnet for å bryte ned plast. Dette ble gjort ved å isolere og identifisere 11 isolater fra jordprøver samlet inn fra seks forskjellige steder i Norge. Ytterligere fem arter som litteraturen har rapportert å ha lavdensitetspolyetylen (LDPE) degraderende egenskaper ble valgt fra stammesamlingen til Veterinærinstituttet (*Mykoteket*). De 16 isolatene ble inkubert i et flytende medium med LDPE-testobjekter i 30, 60 og 90 dager ved 20 °C for å observere muggsoppenes potensial for å bryte ned LDPE-plast. Forsøket ble utført i to paralleller, med og uten glukose. Etter inkubering ble vekten av LDPE-testobjekter og frysetørket muggsoppbiomasse registrert, og testobjektene ble analysert med SEM, ATR-FTIR. SEM-bildene viste potensielle tegn på biologisk nedbrytning i tre av muggsoppisolatene inkubert i 90 dager, ettersom sprekker og ruhet ble observert på overflaten av testobjektene. Ingen endringer i testobjektene ble observert ved ATR-FTIR,i den frysetørkede biomassen eller testobjektets vekttap, uavhengig av tilstedeværelse av glukose, isolat eller inkubasjonsperiode. Resultatene er imidlertid ikke entydige i forhold til soppisolatenes evne til å bryte ned LDPE. Basert på erfaringer fra denne pilotstudien er det anbefalt å optimalisere studiedesignet og metoden før videre forskning på plastnedbrytende muggsopp funnet i norske miljøer utføres.

Abbreviations

ATR-FTIR	Attenuated Total Reflection Fourier Transformed Infrared
SEM	Scanning Electron Microscopy
PCA	Principal Component Analysis
MSM	Mineral Salt Media
ITS	Internal Transcribed Spacer
tef1	Translation Elongation Factor 1 – alfa (TEF1-α)
rpb2	RNA Polymerase B subunit II
tub2	beta-tubulin
PET	Polyethylene Terephthalate
HDPE	High-Density Polythylene
LDPE	Low-Density Polyethylene
LLDPE	Linear Low-Density Polyethylene
LDPE TO	Low-Density Polyethylene Test Object
PE	Polyethylene
PP	Polypropylene
PVC	Polyvinyl Chloride
PS	Polystyrene
RIC	Resin Identification Code

Tabel of contents

1 Introduction

Plastic is fantastic. It is sterile, cheap, versatile and convenient. It changed our lives and can now be found everywhere. From your smartphone, food packaging, shoes, neighborhood, in the air and in the stomach of whales (1, 2). Plastic has saturated our environment and is now finding its way into our bodies (3).

The immense volume and diversity of plastics have become an enormous problem. It is estimated that 450 million metric tons of plastic are produced annually and this number is assessed to probably double by 2045 (4). The total weight of plastic now exceeds the overall mass of all land and marine animals (Figure 1)(5). It is estimated that 13 to 23 million metric tons of the plastic waste generated annually (as of 2016) are emitted terrestrially and 19 to 23 million metric tons enter rivers, lakes, and the oceans (6, 7). The plastic waste entering the environment breaks down to micro- and nanoparticles which makes it an irretrievable and irreversible pollutant (7). Plastic associated pollution has already exceeded the planetary boundary by altering vital Earth system processes. In other words, this means that the threshold for future human existence has already been reached (8). So, what is this plastic thing that threatens the whole planets ecosystem?

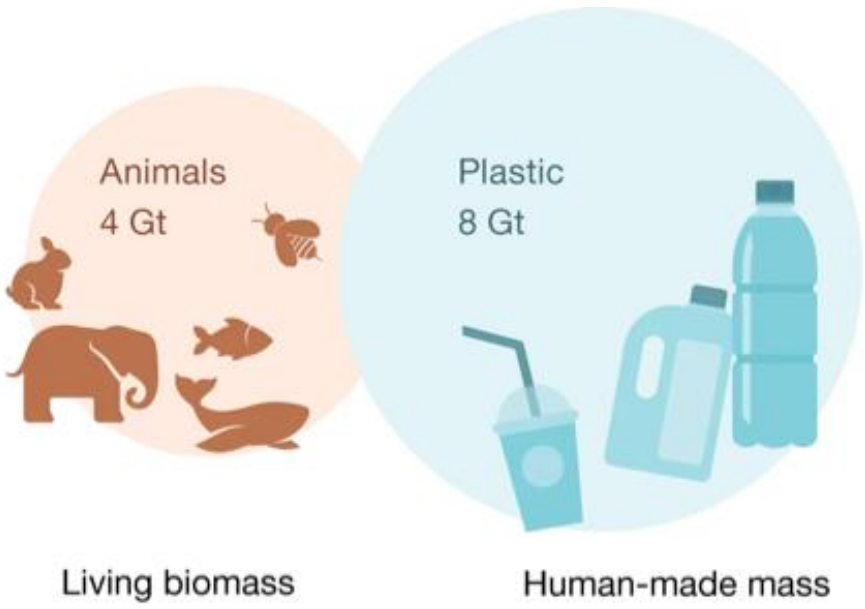

Figure 1. Illustration of the mass ratio between living biomass and Human-made plastic mass represented by circle area. Whitin the plastic estimate is plastic in use and plastic waste. Authors accounted for recycling. The figure is adapted from Elhacham et al. 2020 (5).

1.1 Plastic fantastic?

Plastic is the common term of a wide group of synthetic materials. You encounter multiple of these materials in your daily life, in mobile phones, clothes, packaging, furniture, and cars (and parts of the device on which you may read this thesis) (9). Plastic materials have become ubiquitous, because of the formidable physical and chemical properties of these materials. The origin of the word plastic indicates one of the properties; *plastic* derives from Greek *plastikos* and *plassein* which translates to mold or form (10). Moldability is one of the common properties of this group of materials. Some plastics are soft and flexible whereas others are hard and rock solid.

The attributes of plastics are determined by their composition. Plastics are composed of chemically repeating molecules called monomers which are linked together in long chains forming a polymer (e.g., Figure 2). The different plastics may consist of one or more of these polymers and some additives. Some plastics are plant based (cellulose), but most modern plastics are derived from petroleums like crude oil and natural gas (9).

There are already a significant number of different polymers on the market. With the introduction of co-polymers (more than one type of monomer) and different additives, there is virtually thousands of different combinations and products. Though there are endless possibilities, there are only seven types of plastics that dominate the marked with approximately 90 % of the global demand (11). These are the commodity plastics: Polyethylene Terephthalate (PET), High-Density Polyethylene (HDPE), Low-Density Polyethylene (LDPE), Polypropylene (PP), Polyvinyl Chloride (PVC), Polystyrene (PS) and other plastics (e.g., polycarbonate, polylactic acid, acrylic, and nylon). Figure 2 displays the chemical structure and their Resin Identification Code (RIC). The RIC system was developed by the Plastic Industry Association with the purpose of facilitate recycling of post-consumer plastics but is today of no practical importance as to whether the plastic can or is recycled. It is now administered by American Society for Testing and Materials (ASTM) International (12).

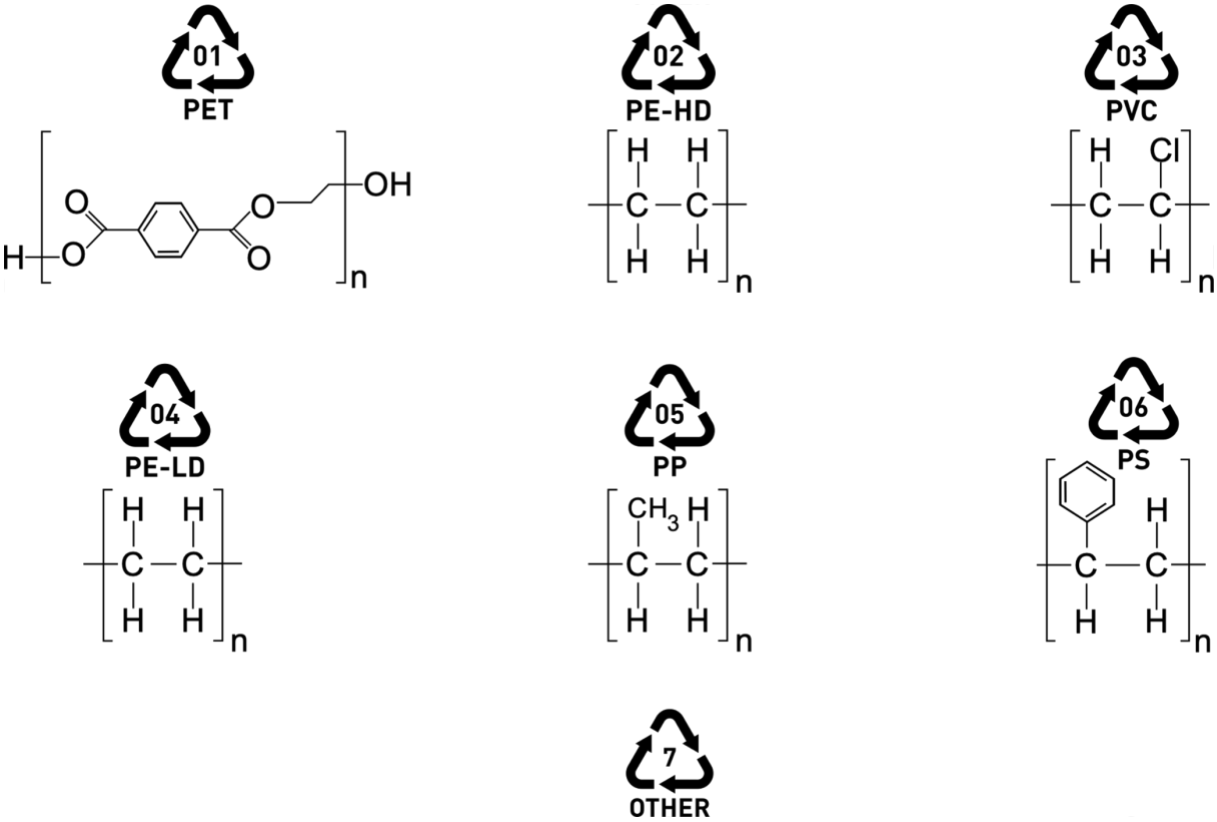

Figure 2. Chemical structure of the monomers for the six most common plastics and the resin identification code for the seven different resins in the RIC-system. From top left the plastics are: Polyethylene Terephthalate (PET), High-Density Polyethylene (HDPE), Polyvinyl Chloride (PVC), Low-Density Polyethylene (LDPE), Polypropylene (PP), Polystyrene (PS) and other plastics.

The commodity plastics have some structural differences which can be grouped into three chemical groups: polyolefins (HDPE, LDPE and PP), aromatic (PET and PS) and halogenated (PVC). As shown in Table 1, these plastics are generally tough, have relatively good resistance against acids, bases, solvents and oils. This hardiness lies at the prime cause of plastic pollution, single-use plastics. A substantial amount of plastic products are used once or a few times before being discarded. Without a proper waste management system, these products end up in local and global ecosystem and persist there.

Table 1. Overview of the most common plastics with some properties and applications. The Polyvinyl chloride is of the hard type without softeners. Asterix (*) indicates that the plastic is resistant against most acids and bases, with some exemptions. The absolute category rating is sorted in decreasing order; good, fair, poor, bad. The table is adapted from Ore et al. (2021) (9).

Plastic	**Density (g / cm^3)**	**Toughness**	**Acid-base resistance**	**Oils and solvents resistance**	**Application**
Polyethylene Terephthalate (PET)	1.3 - 1.4	Fair	Poor against bases	Good	Bottles for consumable liquids, packaging foil, insulation
High-Density Polyethylene (HDPE)	0.93 - 0.97	Good	Good*	Fair against alcohol, acetone, gasoline, aromatic and chlorinated hydrocarbons	Bottles, piping, packaging
Polyvinyl Chloride (PVC)	1.4	Good	Good	Bad against acetone, ethers, aromatic hydrocarbons	Piping, foils, foams
Low-Density Polyethylene (LDPE)	0.91 - 0.94	Good	Good*	Poor against alcohol, acetone, gasoline, aromatic and chlorinated hydrocarbons	Packaging foil, bags, insulation
Polypropylene (PP)	0.9	Good	Good*	Fair against alcohol, acetone, gasoline, aromatic and chlorinated hydrocarbons	Piping, bottles, car interior
Polystyrene (PS)	1.05	Poor	Good*	Bad against acetone, ethers, aromatic hydrocarbons	Single-use products, interior of refrigerator, isolation boards

1.1.1 Polyethylene

As mentioned, PE plastic is one of the most common types of plastic and is ubiquitous in our everyday lives. PE is prepared by polymerization of ethylene monomers (Figure 3). PE can be divided into three main types based on density. Low-density polyethylene (LDPE) is soft and has a density of 0.910 - 0.925 g / cm^3 and melting range of 110 - 115 °C. Medium-density polyethylene (MDPE) is a less common type of medium hardness PE. High-Density Polyethylene (HDPE) has the highest density and melting range compared to the other two at 0.940 - 0.965 g / cm^3 and 130 - 140 °C, respectively.

The PE polymer chains may have a molecular mass of anywhere from 1500 to several million u. Crystalline regions form due to intermolecular interactions between these long chains. The polymer chains for LDPE are somewhat branched, which prevents this crystallization. LDPE has a crystallinity of about 50 %. HDPE, on the other hand, is almost linear and crystalline regions are formed more easily, resulting in a crystallinity of 80 %. Various additives are used in order to give PE products their desired properties. These can be anything from fillers, lubricants, antistatic agents, ultraviolet absorbers to antioxidants. It is this total complexity of plastic as a material which makes it such a difficult problem to deal with. In the current study, two different types of LDPE plastics have been tested due to how common the material is.

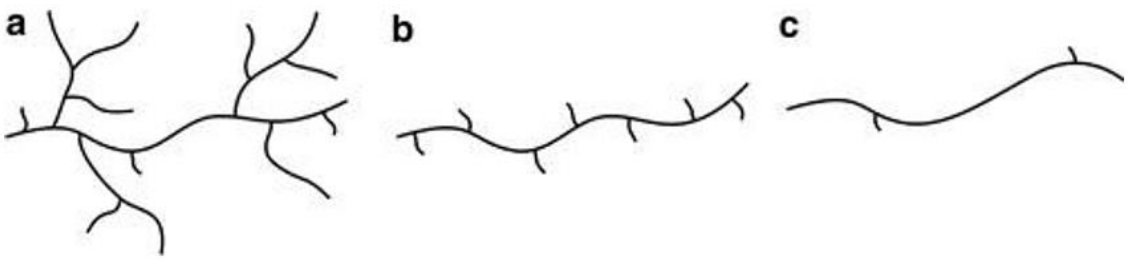

*Figure 3. Illustrating the molecular structure of (**a**) Low-Density Polyethylene (LDPE), (**b**) Linear Low-Density Polyethylene (LLDPE) and (**c**) High-Density Polyethylene (HDPE). The figure is adapted from Okamura et al. (2015) (13).*

1.2 The fates of plastic waste

Plastic products are, in theory, recycled once used or broken. In reality however, the fate of used and discarded plastic is unclear. This is in part due to two things. Firstly, the ubiquity of plastics makes it incredibly difficult to track. The relative amount of plastic of mixed material household objects such as furniture or appliances is not readily available, and therefore difficult to record. Monitoring the massive amounts of plastic discarded at population level, such as food wrappers or miscellaneous items is near impossible to track. Second, is the convoluted bureaucracy that is plastic waste management and recycling.

1.2.1 The bureaucracy of plastic waste

In Norway, it is the responsibility of the local municipalities to collect household waste. This activity is organized by inter-municipal waste companies. Plastic packaging is the primary source of single-use plastics, and therefore the category of plastic products with the highest quality data and tracking after the European Union (EU) directive on single-use plastics (11). Plastic packaging is the primary focus further since it is plastic packaging for there are the most accurate statistics. Plastic packaging such as saran wrap, food containers etc., is collected and recycled by Plastretur AS (14). Plastretur AS is owned by Dagligvarehandelens Miljøforum AS, NHO Mat & Drikke, Dagligvareleverandørenes Forening and Plastindustriforbundet / Norsk Industri (15). These companies also own Grønt Punkt Norge, which operates Plastretur AS. This means that Grønt Punkt Norge directly finances the return scheme, and indirectly operates collection and recycling of plastic packaging. Grønt Punkt Norge is responsible for reporting on plastic packaging collected from households and businesses to the Norwegian Environment Agency (Miljødirektoratet). This confusion of who owns what and what is who's responsibility makes understanding the fate of discarded plastic difficult, but Grønt Punkt Norge has a market share of 98 % (16), and it is these figures that will be discussed. So, what is the fate of 98 % of Norwegian plastic waste?

1.2.2 The ideal fate of plastic waste

In 2021, a total of 138 518 metric tons of plastic packaging was exported from members of Grønt Punkt Norge to the Norwegian market (excluding agricultural plastic). Material recycled after deduction for moisture and process loss comprised 29 % (40 217 tons) (17). The remaining 70 % of plastic waste ends up as energy recycling (incineration), landfill or outside the waste management (lost). According to EUs waste hierarchy (Figure 4), energy

recycling / recovering, and landfill are the least preferred fates of plastic waste. The most desirable waste management strategies are, in descending order, preventing new waste, reusing the waste and material. These priorities are reflected by the American slogan "Reduce! Reuse! Recycle!". The advantage of material recycling is the reduction of the need for new natural resources, not to mention that raw materials based on waste have a lower use of energy than virgin raw materials (18).

Figure 4. The waste hierarchy according to the EU Waste Framework Directive. Preventing waste is the preferred option where landfill (disposal) is the least preferred. The figure is borrowed from the official page on the environmental topic Waste Framework Directive (19).

1.2.3 The real fate of plastic waste

The reasons why most plastic waste is not recycled are many. One recent study on the plastic recycling management in the Nordics (Norway, Sweden and Denmark) points out that the low demand of plastic waste as a secondary raw material throughout the value chain is the key reason. This is primarily due to the fact that oil is still more economically beneficial, but also that the waste management companies have based their system on the incineration of waste which is then used as district heating (fjernvarme) or to generating electricity (20). Burning plastics is still highly polluting, even by modern waste treatment plants (21). Potential

solutions are increased collaboration, public procurement and investment in technology throughout the plastic waste management system e.g. from collection to production of new products (20).

1.2.4 The future of plastic waste

To increase the rate of material recycling, developing new methods for breaking down the different types of plastics into their constituent monomers is crucial to make these processes easier and a more attractive option than incineration for heating or electricity. To understand how it is done as of today we need to define the four categories within recycling of plastics (22):

1. Primary recycling is the mechanical reprocessing of waste into a new product with equivalent properties as the old one and are referred to as closed-loop recycling.
2. Secondary recycling is the mechanical reprocessing of waste into a new product with lower properties compared to the old one and are therefore referred to as downgrading.
3. Tertiary recycling is described as feedstock recycling because it involves depolymerizing the plastic into its chemical constituents.
4. Quaternary recycling is energy recovery by incineration.

In theory all of the thermoplastics (e.g. PET, PE, PP, PS and PC) can get pliable and moldable over and over again by heating the plastic (23). But as of today, it is primarily PET that are closed-loop recycled, where used PET bottles get recycled to new PET bottles. In addition there are some closed-loop recycling of pure HDPE and PVC (22). The other thermoplastics get downgraded to new products with reduced properties. There is therefore a great potential for being able to depolymerize the plastic waste into its monomers which can then be used to make new products with equivalent properties of virgin plastics.

1.3 Microorganisms to the rescue

Microorganisms are already the degraders of nature, with fungi firmly grasping the title of primary decomposers in specific situations (24). In 2016 researchers in Japan published a paper where they had found a bacterium that degraded PET (most efficient against low-crystalline PET film) (25). The news of the groundbreaking discovery of the "Plastic-eating bacteria" went international. The bacterium's taxonomic nomenclature is *Ideonella sakaiensis* and it originated from samples collected at a PET bottle recycling site. *I. sakaiensis* secretes the key enzymes PETase and MHETase, which are the two enzymes responsible for hydrolyzing PET to its constituent components terephthalic acid and ethylene glycol (25). In the last 20 years, many more microorganisms have been described to degrade PET and other types of plastic than just *I. sakaiensis* (26, 27). Other enzymes associated with plastic degrading are cutinases, lipases, proteases, esterases, laccase and peroxidases (28).

Several of the promising microorganisms that may possess plastic degrading properties are fungi (28). Some examples of fungal species associated with degradation of PE plastic are *Pencillium simplicissimum*, *Aspergillus niger*, *Aspergillus japonicas* and *Fusarium* sp., *Aspergillus terreus* and *Aspergillus sydowii*, *Trichoderma harzianum*, *Penicillium chrysogenum* and *Penicillium oxalicum* (28-31). There is a need to include fungi in order to understand the mechanisms involved with biodegradation, especially considering that fungal biodegradation associated enzymes often have higher activity compared to bacteria (32).

1.4 Unlimited power with fungi

Fungi is a kingdom of eucaryotic organisms without chlorophyll and are therefore heterotrophic (*hetero* (Greek) meaning “another”; *troph* (Greek) meaning “nourishment” or “food”). They can live as parasites on animals and plants or as saprotrophs decomposing dead organic matter. Fungi can also form mutualistic relations with green algae and / or blue-green bacteria (lichens) and with plants in mycorrhiza (33).

Phylogenetically fungi are closer related to animals than plants. Some of the similarities between fungi and animals are glycogen, chitin and collagen. Ergosterol is an important component in fungal cell membranes, which animal cell membranes do not contain. Fungi do not have an internal digestive system like animals, but relay on diffusion or transport of nutrients through the cell membrane (33, 34).

Filamentous fungi grow with cylindrical threadlike structures called hyphae. New hyphae are generated by branching, which are the formation of new hyphal tips along existing hyphae. When an expanding tip encounter another hypha, these may fuse together and form intricate networks with different origins. This mechanism, anastomosis, allow the fungus to share nutrients and communicate across the whole hyphal network. Anastomosis can occur with self-exploring hyphae, or a different compatible fungus. Hyphae can be divided into compartments by cross walls (septa). These septa have pores that allow transportation of nutrients and organelles. The interconnected network of hyphae forms the mycelium (34). Non-filamentous fungi such as yeast are not discussed in this study.

Identification of organisms is important for distinguishing one organism from another and at the same time communicating unambiguously with other scientists. Morphological and molecular identification of the fungal species was used in this study.

1.4.1 Morphological identification of fungi

The taxonomy of fungi is a laborious process as there is enormous diversity within the fungal kingdom. For the sake of simplicity and the goal of this thesis, the morphological identification was restricted to the genus level of three genera *Aspergillus*, *Penicillium* and *Trichoderma*.

The recommended conditions when cultivating for morphological identification of *Aspergillus* is a three-point inoculation on Malt Extract Agar (MEA) and Czapek Yeast autolysate Agar (CYA) incubated at 25 °C for 7 days. Incubation at other temperatures such as 37 ° C and other media such as species-specific media or media with higher sucrose concentration may be helpful.

Aspergillus often grows fast with pigmented conidia that give the colonies colors such as black, brown, tan-yellow, several shades of green, yellow, pink or white. When looking through a stereo microscope, the conidiophore of *Aspergillus* might be reminiscent of a lollipop. Conidiophores are often aseptate and have unbranched stipe (main axis) which ends in an enlarged vesicle at the end of the apex (Figure 5 – A). The phialides can be attached directly to the vesicle or to a metulae, where the phialides carry conidia in chains. Conidia are single-celled, hyaline or pigmented, and with a smooth or ornamented surface. The chains of conidia can radiate across the entire vesicle or form dense columns.

For identification of *Penicillium* a three-point inoculation on CYA and MEA incubated in dark at 25 °C for 7 days is recommended. Additional media and growth rate testing at 30 °C and / or 37 °C may be required. The colonies in shades of green or whites and have commonly a surface texture similar to velvet. Conidiophores are hyaline colored and smooth- or rough-walled. The main axis (stipe) of the conidiophore may be branched with metulae (branches with a whorl of phialides). The branching pattern is important in identification. The phialides are often bottle-shaped and produce long chains of conidia in various forms (globose, ellipsoidal etc.). Conidiophores of *Penicillium* are often compared to paintbrushes (Figure 5 – B).

It is recommended to grow presumptive *Trichoderma* on MEA at 25 °C with dimmed daylight or near-UV light. It is further recommended to inspect the cultures after 5 days of incubation. The colonies grow rapidly and appear as hyaline colored or in several shades of green. Conidiophores can form tufts that can be distributed in concentric rings. The sides of the colonies are often white or with hints of yellow (depending on the medium and species). The conidiophore main axes are highly branched, which then form side branches. From the branches spring the phialides (often bottle-shaped), which then carry the conidia. The conidia are often smooth (may be rough) and sub-globose to short ovoid in shape. The conidiophores of *Trichoderma* are often described as bush-like (Figure 5 – C).

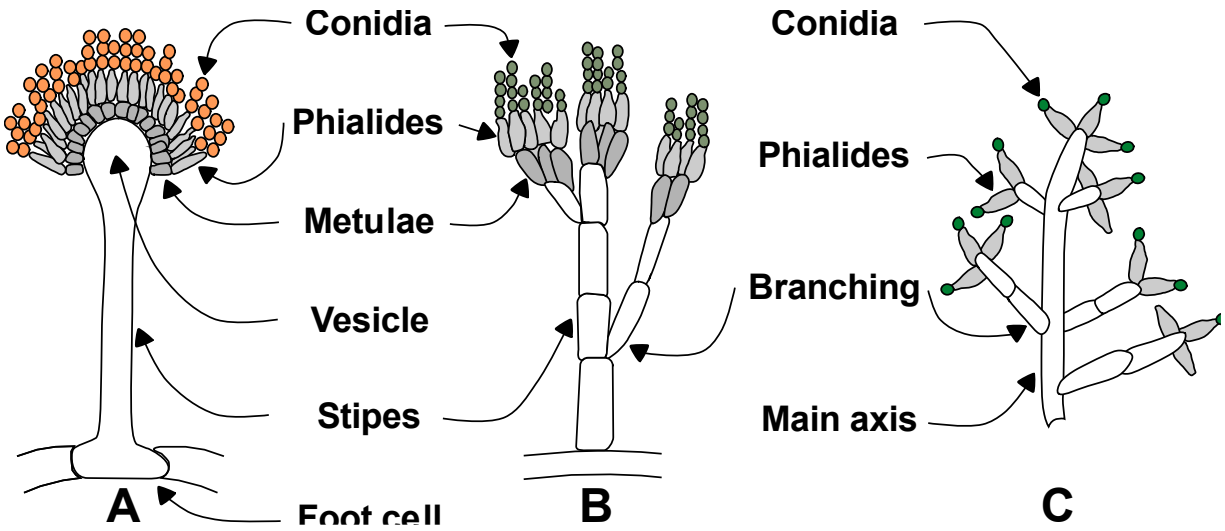

*Figure 5. Simplified representation of spore-forming structures (conidiophores) for three of the species used in this study. The three species are Aspergillus terreus (**A**), Penicillium chrysogenum (**B**) and Trichoderma harzianum (**C**). The presentation is based on drawings and microscopy images from Samson et al. 2019 (35).*

1.4.2 Molecular identification

An alternative or addition to identifying microorganisms by their morphology, is identifying at the molecular level. This involves both identifying metabolites and using genetic tools. The molecular genetic identification techniques used in microbiology are whole-genome sequencing of an organism, multiple gene sequencing (pathogenic or housekeeping genes) and singular gene sequencing, such as the 16S rRNA gene in bacteria or the Internal Transcribed Spacer (ITS) in fungi (36). Molecular identification will in several cases also be the only possibility for identification at species level, as for several species within the genus *Trichoderma* (37). Central to all of these techniques is the analysis of Deoxyribonucleic Acid (DNA).

Molecular identification was done by amplifying, sequencing and then searching for sequences similarity in a database. ITS and Translation Elongation Factor 1 – α (*tef1*) were used as molecular markers in this study. Large amounts of DNA are needed for good quality analyzes. The main function of polymerase chain reaction (PCR) is to make copies of (amplify) a specific sequence of DNA. This amplification of DNA depends on a cycle of four steps repeated a number of times 20 – 40, where DNA gets replicated by the enzyme DNA polymerase and a set of nucleotide sequences (primers) complementary to the flanks of the DNA segment of interest. A final component that is critical for synthesizing the new DNA strand is deoxynucleotide triphosphate (dNTP), where nucleotide is the collective term for the four different nitrogenous bases: adenine, guanine, cytosine and thymine (dATP, dGTP, dCTP and dTTP, respectively). The PCR process involves 4 steps (38):

1. Initialization: The reaction is heated to 94 – 96 °C for 2 – 10 minutes to activate the DNA polymerase and to denature possible contaminants
2. Denaturation: The hydrogen bonds between the double-stranded DNA are broken by heating the reaction to 94 – 98 °C for 20 – 30 seconds
3. Annealing: When the DNA is denatured into single strands the reaction temperature is lowered to 50 – 56 °C for 20 – 40 seconds and the primers bind to their complementary sequences on each single stranded DNA template.
4. Elongation: After the primers are annealed, these primers guide the DNA polymerase enzyme to synthesize a new DNA strand by incorporating dNTPs in the 5' – 3' direction. The optimal reaction temperature for the polymerase is 72 – 78 °C for 30 – 60 seconds.

The temperatures and time interval given are examples and may vary based on the selected DNA polymerase, primer and length of the amplicon. Steps two to four make up the majority of cycles and are repeated for the desired number of times, which is usually from 25 – 35 cycles. After each cycle, the number of DNA strands is doubled, which generates $2^{40} = 1.1 \times 10^{12}$ after 40 cycles of one original DNA strand. After a certain threshold unspecific amplification takes place, which is the random amplification of non-target DNA. At the end of the last cycle there is a final elongation step that keeps the reaction at 72 – 78 °C for 5 – 15 minutes. This step ensures that any remaining single-stranded DNA is fully extended after the last PCR cycle.

Sanger sequencing is a technique often used to determine the DNA sequences of molecular markers. The replication reaction itself is very similar to PCR, where it consists of a DNA template, a DNA primer, DNA polymerase and dNTPs. In contrast to PCR, modified di-deoxynucleotide triphosphates (ddNTPs) are also used, which is an analog of dNTPs. These ddNTPs lack an -OH group at the 3' end which prevents the DNA polymerase from forming phosphodiester bond to the next dNTP / ddNTP (Figure 6). The incorporation of the analog leads to the termination of the growing strand. The ddNTPs are also labeled with fluorescent molecules, different color for each ddNTP (38, 39).

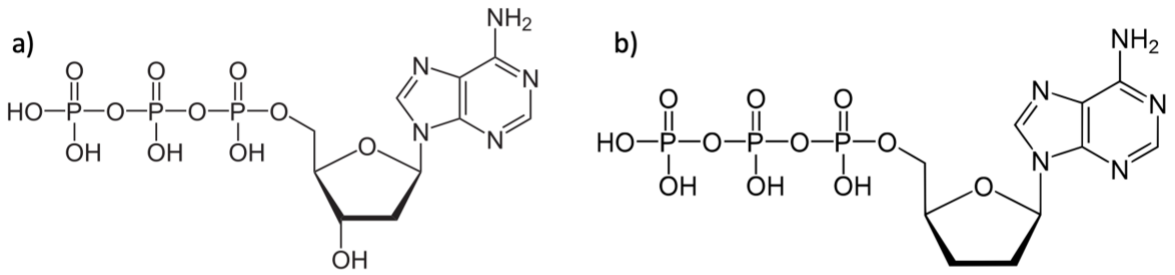

*Figure 6. Idealized presentation of the molecular structure of (**a**) deoxyadenosine triphosphate (dATP) and (**b**) dideoxyadenosine triphosphate (ddATP) used in Sanger sequencing. The missing 3' -OH of the ddATP inhibits elongation of the growing strand. Figure adapted from Wikimedia Commons.*

This reaction mix undergoes cycles with varying temperatures approximately to a PCR program. This results in the formation of a series of DNA fragments that all have the same primer start but with different lengths. The DNA fragments are then separated by capillary electrophoresis (38). The capillary is a tube with a small cross-section filled with a separation matrix of cross-linked polymer (40). The mechanism of separation is the same as for agarose gel electrophoresis, where the negatively charged DNA fragments will migrate from a negative pole (cathode) to a positive pole (anode). The DNA fragments are separated on the basis of size, where smaller fragments will move faster relative to larger fragments (41). A laser is mounted at the end of the capillary which then excites the fluorescent molecules on the ddNTPs through a window in the capillary. The DNA base sequence is recorded with a detector that measures the emitted light and where the product is a chromatogram (also called an electropherogram) (38, 39).

1.5 How to determine fungal biodegradation of Polyethylene

There are several methods to determine if there are any changes in the plastic material after incubation with fungal isolates. In this experiment measurements of freeze-dried biomass and weight loss in the LDPE test objects were used, as well as analysis by Attenuated Total Reflection Fourier transform infrared spectroscopy (ATR-FTIR) and scanning electron microscopy (SEM). It is important to acquire a basic understanding to understand the choice of the latter two methods of analysis.

1.5.1 Infrared spectroscopy

As polyethylene (PE) breaks down, it oxidizes. A frequently used method for measuring oxidation and the accelerated aging of PE is infrared (IR) spectroscopy. IR spectroscopy includes many different types of instruments, sample preparations and results treatments. There is, as of yet, no standard procedures established for IR spectroscopy analyzes of PE (42).

Spectroscopy is a technique that uses electromagnetic radiation (EMR) to study the chemical composition or structure of a material. This is possible due to how different molecules and compounds interact with EMR. EMR interacts with molecules, yielding electromagnetic spectra that differ depending on the wavelength of the EMR and the characteristics of the molecules analyzed. The electromagnetic spectrum can be divided into eight generalized groups (in order of increasing wavelength): gamma rays, X-ray, ultraviolet (UV), optical light (Vis), IR, microwaves, radio waves and long waves (Figure 7). If a molecule is exposed to: X-rays, UV and Vis it can result in changes in electronic states, IR (and in part transient to Vis and microwaves) can lead to changes in the rotation and vibration states of molecules, while micro- and radio waves can change the rotational states of electron spin and nuclear spin, respectively (38). All these properties are utilized by various techniques and instruments, but only IR spectroscopy used in this study.

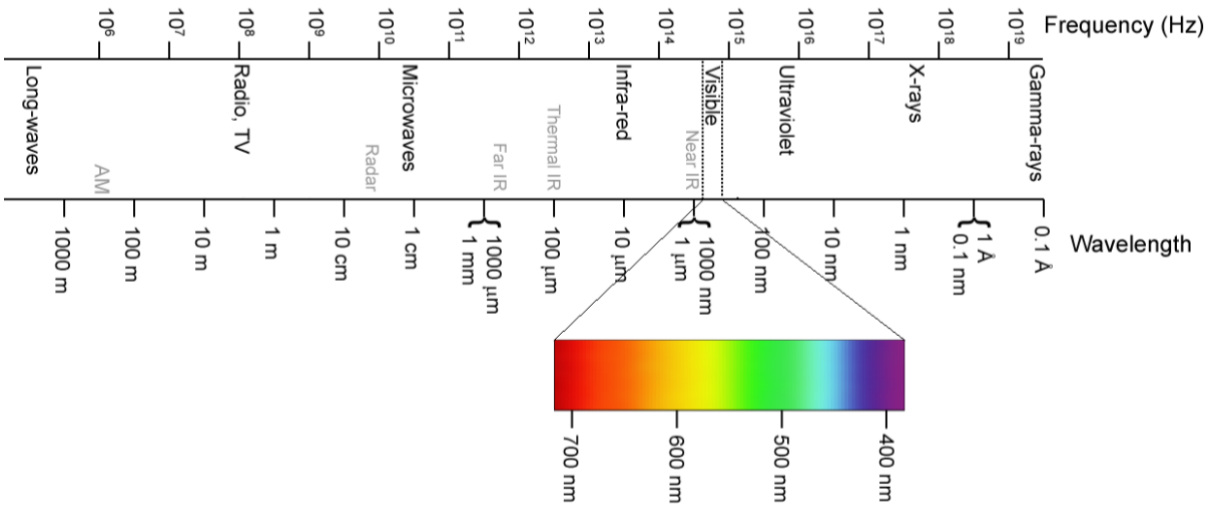

Figure 7. An illustration of the full electromagnetic spectrum. Adapted from Wikimedia Commons.

In short, IR spectroscopy is the study of interaction between any kind of organic or inorganic matter and infrared radiation. IR encompasses the wavelengths between 700 nm and 25 000 nm, which means that it is longer than visible light but shorter than microwaves. Depending on the wavelength, the IR can be subdivided into near, mid and far infrared. The mid IR spectrum (MIR) is the most commonly used when performing IR spectroscopy. Wavelength or frequency as a unit of measurement are not used in IR spectroscopy, but wavenumber. Wavenumber is defined as the number of wavelengths per unit distance, typically centimeters (cm^{-1}) (43). This means that as the frequency and energy increase, so does the wavenumber, while the wavelength decreases.

IR spectrometry is based on the concept of absorption of energy by molecules. As the molecules are exposed to IR radiation, they absorb its energy and then transition to a higher level of vibration. This can best be explained by imagining that all bonds between atoms in a molecule consists of springs. A spring can be bent and stretched, which is precisely why these vibrational states have been given this terminology. The vibrational modes caused by IR light are shown in
Figure 8, and can either be stretching (symmetric and asymmetric) or bending (deformation) like twisting, rocking, wagging and scissoring vibrations. When a molecule absorbs the incoming (incident) light of a specific wavelength, this wavelength will then be missing in the passing (transmitted) light. This is measured as an absorption band in the registered spectrum (44).

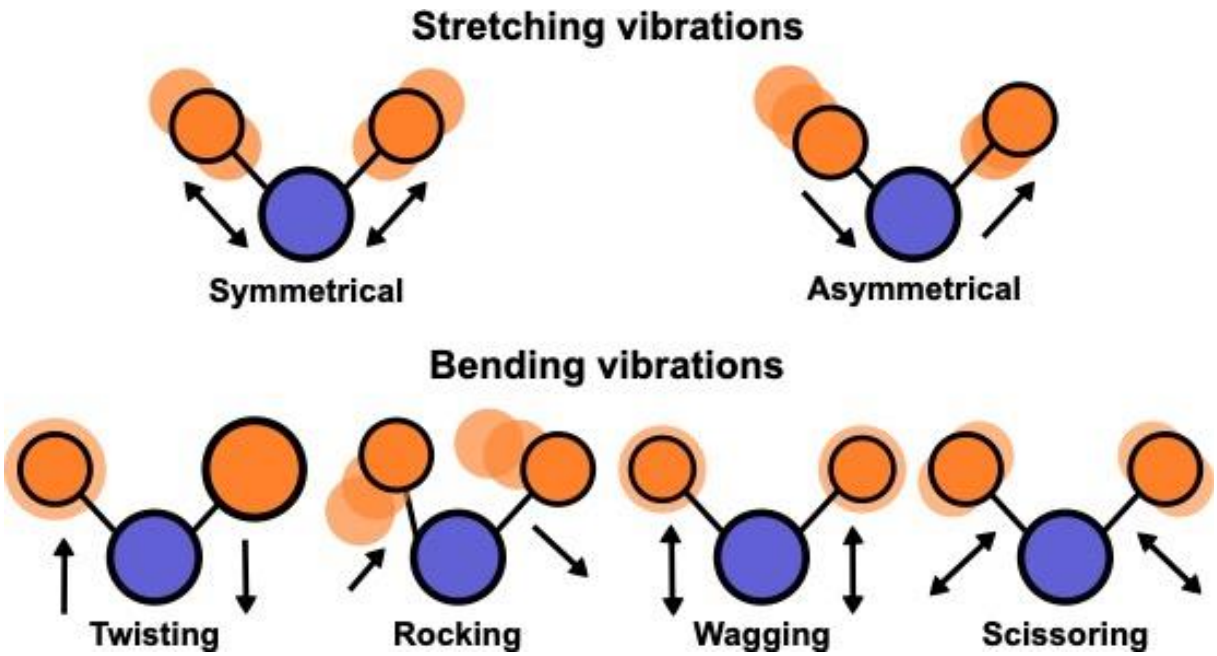

Figure 8. The two categories of molecular vibrational modes. Stretching vibration that may either be symmetrical or asymmetrical stretching. Bending vibration that may either be twisting, rocking, wagging or scissoring. The figure is adapted from Ozaki et al. (2020) (44).

Conventional IR spectroscopy uses monochromatic light which then passes through the sample, which is then recorded as a transmission spectrum. This means that in order to measure the absorbance at the given wavelength, the sample must be irradiated by only a single wavelength (monochromatic) at a time. A development of this method replaces the monochromator with an interferometer where the raw data must pass through the mathematical algorithm Fourier transformation, which gives us Fourier transform infrared (FTIR) spectroscopy. FTIR typically uses a Michelson interferometer, which is a set of mirrors where one has a fixed position, and the other is movable. By changing the position of the moving mirror, one will be able to form wave interference (constructive and destructive). This makes it possible to irradiate the sample with several wavelengths at the same time, where the different positions of the mirror generate different spectra. The raw data (in the form of an interferogram) is therefore a product of light absorbed at each position the mirror had, which is not very informative. Fourier transform converts this to wavenumbers (38, 44).

FTIR has three advantages over conventional IR. First, higher signal-to-noise ratio due to the fact that several wavelengths are collected simultaneously (Fellgett's advantage (45)). Second higher throughput due to the light not being dispersed and then restricted by a slit that prevents unwanted light to pass (Jacquinot's advantage). Third better wavelength accuracy due to the interferometer being calibrated with a laser of known wavelength as opposed to a monochromator (Connes' advantage) (46).

The procedure depends on sample preparation regardless of whether traditional IR or FTIR spectroscopy is to be performed. If gas, liquid or solids are to be analyzed, this requires different sample preparation routines, all of which present their challenges (e.g., liquid cells and KBr pellets). To avoid complex and time-consuming sample preparation procedures, a supplement to the FTIR called Attenuated Total Reflection (ATR) has been developed (46).

A common accessory of FTIR spectrometers is an ATR mode, which is an extension of the FTIR instrument setup. To collect an ATR spectrum, one needs a suitable IR light source, an ATR crystal, and a detector. Of these parts, the choice of crystal, typically a diamond, germanium or zinc selenide crystal, is the most critical. The crystal material must have a higher refractive index than the sample investigated and be resistant to chemical and mechanical stress. Diamond crystals are a very good all-rounder as it satisfies these criteria even if it is somewhat expensive. To collect a spectrum the sample is placed undiluted on the ATR crystal and then pressed against the crystal if it is a solid sample. The IR light enters the crystal at a given angle of incidence where the light is then totally reflected back into the crystal at the interface between the crystal and the sample (Figure 9). Some of the energy of the IR light will interact with sample material at the interface due to the evanescent wave phenomenon. This transition of energy into the sample results in a weakened IR light (attenuated). The sample material is penetrated only in the top surface by the evanescent wave (maximum 2 μm). After at least one internal reflection the light is collected by a detector. It is especially important to ensure good contact between solid samples and the crystal to remove ambient air and at the same time ensure good energy transfer. For liquid samples, it is sufficient to apply this over the crystal. Spectra from ATR-FTIR are the result of different vibrational modes from the given molecules and are often given as an absorption spectrum (38, 46). An overview of absorption peaks for different types of PE is presented in Table 2.

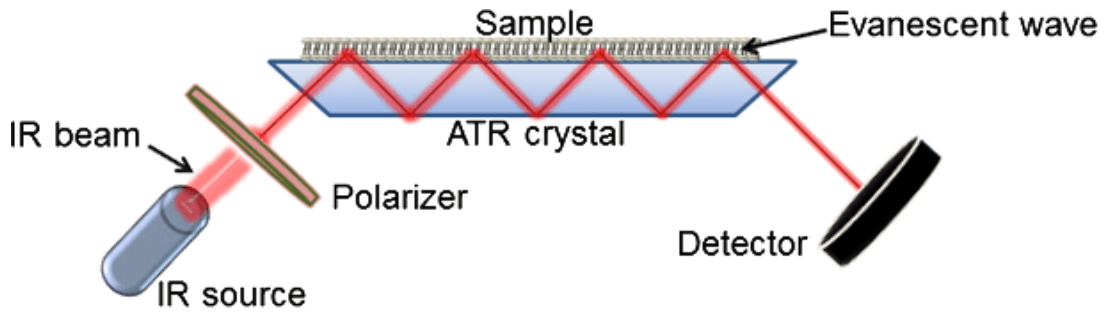

Figure 9. Schematic illustration of an Attenuated Total Reflection Fourier Transformed Infrared (ATR-FTIR) system. An infrared (IR) beam passes through the ATR crystal with the sample on top. The evanescent wave penetrates into the sample which then interacts with molecules in the surface of the sample material (causing different vibrations modes) and is absorbed by the sample. The polarizer filter the IR beam of mixed polarization into a beam of well-defined polarized IR beam. Figure borrowed from Ausili et al. (2015) (47).

Table 2. Fourier Transformed Infrared absorption spectrum peaks of different polyethylene types based on Brian C. Smith's (2021) publication (48). The peaks are given in wavenumber (cm^{-1}).

Vibration	**HDPE (cm^{-1})**	**LDPE (cm^{-1})**	**LLPDE (cm^{-1})**
CH_2 Asymmetric Stretch	2919	2917	2915
CH_2 Symmetric Stretch	2850	2852	2847
CH_2 Scissor	1472	1471	1472
CH_2 Scissor (split in crystalline samples)	1464	No peak	1463
C - CH_3 Symmetric Bend (umbrella mode)	No peak	1377	1378
CH_2 Rocking	730	718	729
CH_2 Rocking (split peaks in crystalline materials)	720	No peak	719

1.5.2 Electron microscopy

Biodegradation of plastic due to microorganisms is frequently studied by scanning electron microscopy (SEM) that allows for a high-resolution study of the materials surface. Electron microscopy is a technique that has many common features with ordinary light microscopy, but with the significant difference that electrons are used instead of light. Light microscopes are limited in resolution due to the wavelengths of optical light (EMR). The resolution cannot be less than half the wavelength. Electrons have a wavelength that is 1 / 100 000 of the wavelength of optical light, hence electron microscopes can achieve a much higher resolution and magnification than light microscopes (49).

The structure of a SEM is similar to that of a light microscope (Figure 10). It needs a radiation source, which in this case is an electron gun instead of an incandescent bulb. Electrons are emitted from a resistance-heated needle-shaped tungsten wire. The tungsten wire (cathode) is given a high negative electrical potential relative to an anode located a little further below the tungsten filament. The anode is positively charged and will attract the negatively charged electrons into the instrument column. Lenses are used to focus the electron beam. These lenses are not made of glass as in light microscopes but are instead electromagnets. The electromagnets can affect the electron beam through magnetic and electrostatic fields. The electron beam is first collected by a condenser lens, then focused to the final beam size (probe) by an objective lens. The electron probe is now ready to be swept over the sample (38, 50).

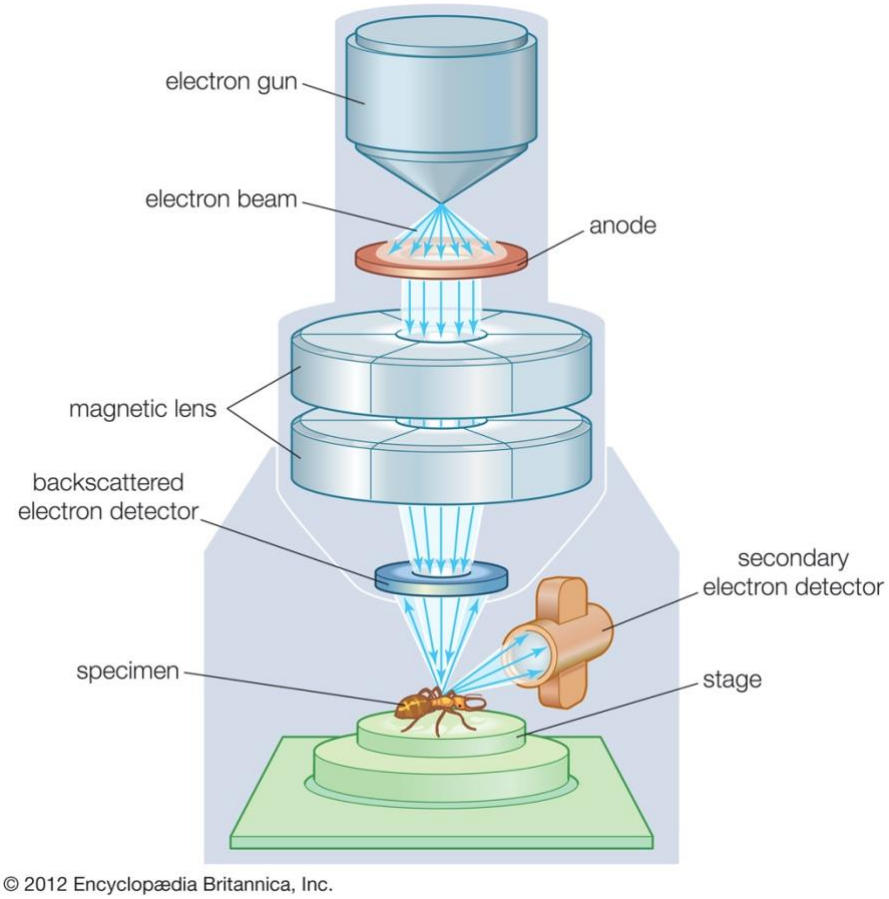

Figure 10. Schematic representation of scanning electron microscopy (SEM). An electron gun emits an electron beam which is accelerated towards the anode. The electron beam is then passed through two magnetic lenses which results in a highly concentrated electron beam (probe) which is aimed at the sample. Electrons from the probe then interact with atoms in the sample surface resulting in different signals. Backscattered electron detector and secondary electron detector are examples of two types of detectors that are often used. The signal is then processed and displayed on a monitor. The figure is borrowed from Joy et al. (2019) (51).

When these primary electrons (PE) hit the sample material, several types of signals can be emitted from the sample material, where secondary electrons (SE), backscattered electrons (BSE), and X-rays are the most common. Of these, SE provide information about the surface (topography), while BSE and X-rays provide information about the chemical composition of the analyzed material (38). SE is formed by PE colliding with an electron from an atom in the sample material. PE then knocks out this electron (SE) which can then be detected by a positively charged detector (Figure 11). BSE are electrons that do not collide with either atomic nuclei or electrons but are thrown back towards the surface of the sample material. Heavier atoms in the sample will result in more BSE relative to lighter atoms. X-rays can be emitted by PE colliding and removing an electron from one of the inner shells of atoms in the

sample. This results in an electron with higher energy taking up the space and at the same time releasing energy. The energy in the form of X-rays is characteristic of each element (52).

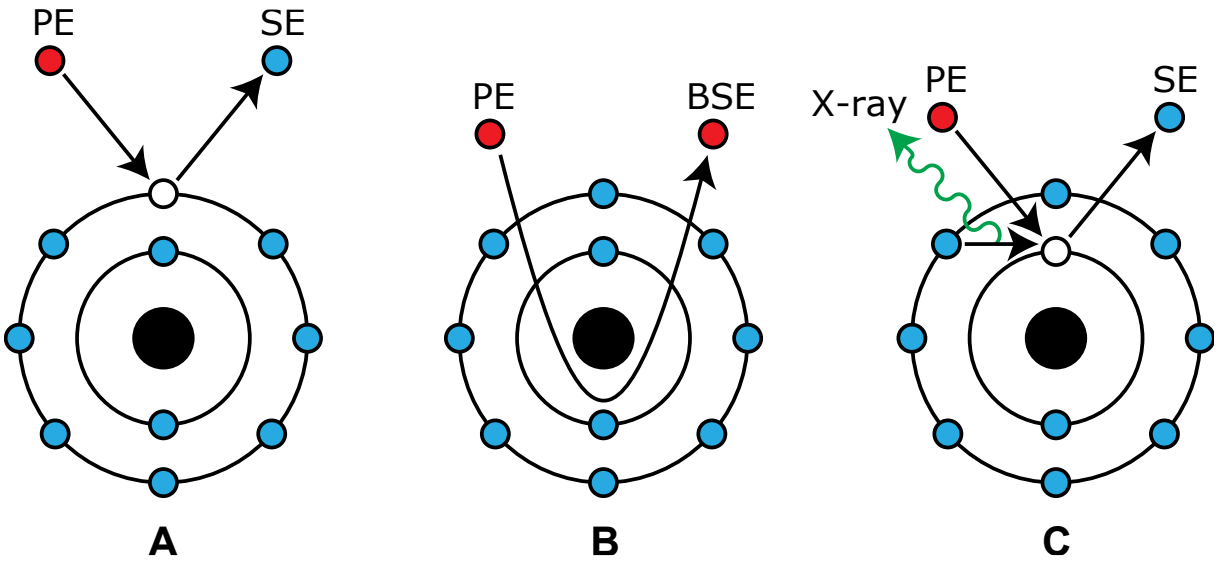

*Figure 11. Schematic representation of the interactions between the electron beam (primary electrons, PE) and the sample material. Blue dot, white dot, black dot and green arrow are electrons, knocked out electrons, atomic nuclei and emitted X-rays, respectively. Different SEM images are formed based on the different emitted signals of (**A**) secondary electrons (SE), (**B**) backscattered electrons (BSE) and (**C**) characteristic X-rays. The figure is borrowed from Wikimedia Commons and adapted by the author of this study (53).*

There are several factors that must be considered when analyzing biological samples with SEM. To avoid the electron beam colliding with particles in the air, which will disturb the electron beam, it is necessary to carry out the analysis in a vacuum. Water evaporates in a vacuum, and hence sample material containing water must be dehydrated. Dehydration of biological samples often leads to collapse and changes in the sample matrix. This can be avoided by chemical fixation of the sample. Fixatives such as glutaraldehyde and formaldehyde stabilize and preserve the structures in the sample by forming intermolecular bonds between proteins. After fixation and dehydration in an ethanol series with increasing alcohol content, the ethanol is replaced with liquid carbon dioxide in a critical point dryer. Finally, the carbon dioxide must be removed also, which is achieved by phase transition to supercritical fluids. The sample material is gently heated past the critical point (according to the phase diagram) after which the pressure is gradually reduced by venting the gas. The result is a completely dry sample material (38, 50).

The sample material to be examined must also be able to conduct electricity to prevent the sample material from accumulating electrons resulting in charging. Charging the sample material will result in distorted signal and poor images. To make biological samples electrically conductive, the samples are coated with a thin layer of gold, palladium or an alloy of these via a sputter coater. Sputter deposition is a vacuum system in which supplied argon atoms (or another inert gas) loose an electron due to a strong electromagnetic field. This results in the argon atoms being positively charged, forming plasma. The source of the gold / palladium alloy (called target) is negatively charged, which causes the ionized argon atoms to bombard it and release gold / palladium atoms. These gold / palladium atoms are thrown out and hit the sample material (called substrate) (54). The desired thickness of the cover layer is achieved by measuring the thickness or carrying out the process at a set time. The sample material is then mounted on a stub with carbon adhesive tape and is finally ready for examination by SEM (38).

1.6 Aim and relevance of this study

Norway is obliged through the EEA (EØS) agreement to implement the EU's Packaging and Packaging Waste Directive (part of the circular economy package) in order to reduce the amount of plastic waste while recycling more (55). This means that the new targets for material recycling of plastic packaging waste are 50 % by 2025 and 55 % by 2030 (56). This study can contribute to knowledge about microbial degradation of plastic.

Knowledge acquired from this study can be used in accordance with several of the United Nations (UN) sustainable development goals (SDG) (57). SDG no. 12: Responsible Consumption and Production includes circular economy and recycling. SDG no. 13: Climate Action deals with acting immediately to combat climate change and its consequences. SDG no. 14: Life Below Water includes preserving the natural ecosystem and reducing plastic in the oceans, and SDG no. 15: Life on Land deals with protecting the ecosystem and species diversity on land. This study can contribute to these sustainability goals by finding new economically viable methods for dealing with the increasing amount of plastic waste towards a future circular economy (Figure 12).

Figure 12. The four UN sustainable development goals which this study can contribute to (57).

The primary goals of this study are to **identify fungi from Norwegian environments that can degrade plastic and acquire practical experience in the field of plastic biodegradation**. This was done by isolating fungi from soil samples collected from different places associated with plastic handling in Norway, and then cultivate these in accordance with current literature to investigate plastic degrading properties. The type of plastic that this study focused on was LDPE due to it being highly common. Analysis by ATR-FTIR, SEM and measurements of weight and freeze-dried biomass were used to investigate plastic samples for degradation.

2 Materials & Methods

2.1 Soil sampling and isolation of fungal strains

A total of 15 soil samples were collected from six different locations. From Valdres, a total of 10 samples were collected from two different private silage bale polywrap waste sites (lagringsplass for rundballeplast) (approximately 670 meters above sea level), at the intermunicipal renovation (Valdres kommunale renovasjon, VKR, approximately 530 meters above sea level) and on Valdresflye (1389 meters above sea level). The Valdres samples were collected from 2-15 cm beneath the turf and stored in 2 dL sterile plastic containers at room temperature. Additionally, five samples were collected from the Follo region: Bølstad recycling station (Ås, lokalitet 437 i grunnforurensningsarkivet, approximately 670 meters above sea level) and Paddetjern (Nordre Follo, lokalitet 418 i grunnforurensningsarkivet, approximately 240 meters above sea level). The Follo samples were collected from 1-30 cm beneath the turf and stored in sterile plastic bags at room temperature. These sites were selected primarily based on the hypothesis that exposure of fungi to plastic (i.e., storage of plastic waste) could perhaps result in natural adaptation where the fungi develop the ability to use plastic as a carbon source and subsequently degrade it. This is also supported by scientific literature where several microorganisms with plastic degrading potential have been found from plastic waste management sites (25, 29). Valdresflye was chosen based on the fact that via bioprospecting interesting fungi have been found high above the sea in Norway earlier (58).

Isolation of fungi from the soil samples were done by serial dilution and plate spread technique. Soil suspensions were made by applying 1 g of soil sample to 9 g of 0.9 % NaCl physiological saline solution. The suspension was vortexed briefly, and then left for 30 minutes for sedimentation of large particles. Without disturbing the sedimentation, 1 mL of the soil suspension was diluted with 9 mL of 0.9 % NaCl physiological saline solution to make a 10^{-2} dilution. This was further 10-fold serial diluted until reaching a dilution factor of 10^{4}. Each serial dilution was vortexed before being further diluted. The suspensions were inoculated on ½ strength Potato Dextrose Agar (PDA, see Appendix 6.1 Culture Media), Malt Extract Agar (MEA, see Appendix 6.1 Culture Media) and Dichloran glycerol agar (DG18, see Appendix 6.1 Culture Media) with 100 µL of 10^{-3} and 10^{-4} dilutions and spread with a Drigalski spatula. The Petri dishes were incubated at 25 ± 1 °C for 5 days.

After 5 days of incubation colonies of filamentous fungi were selected, isolated, and inoculated on new PDA petri dishes with a platinum inoculation loop. The selection criterium was rapid growth rate. A second isolation step was performed where necessary to achieve axenic culture.

2.2 Preparation of Low-Density Polyethylene Test Objects

To test the LDPE degrading potential of fungal isolates three different groups of LDPE test objects (LDPE TOs) from two different sources were prepared. The shape and choice of thickness was selected to optimize surface area and handling. The three groups of LDPE TOs were prepared from a 1 mm thick LDPE sheet (Goodfellow, Huntingdon, UK) and 0.06 - 0.09 mm thick minigrip® LDPE zip-bags (JOKA packaging, Hørsholm Denmark). Discs of 5 mm in diameter were punched manually from the 1 mm thick sheet (LDPE TO 1) and from the zip-bags (LDPE TO 2). The last test object group was 40 x 4 mm “rods / sheets” and were also prepared from the zip-bags (LDPE TO 3).

For sterilizing and potential induction of small-scale oxidization, LDPE TOs were UV-radiated at 234 nm wavelength with a distance of 60-80 cm from the UV-source for 24 hours. LDPE TOs were then collected and stored in sterile petri dishes at room temperature.

2.3 Morphological identification of fungal isolates

Macro- and micromorphology were used for fungal identification along with molecular identification.

2.3.1 Fungal culturing

Fungal isolates were maintained on ½ PDA and recultivated every second month. This was done by gently touching fungal mycelia with a sterile platinum inoculation loop followed by inoculation in the middle on a new agar plate. The newly inoculated agar plates were then incubated in perforated plastic bags in room temperature. The platinum inoculation loop was sterilized by dipping the wire in 90 % ethanol and passing it through the flame of a Fireboy (INTEGRA biosciences, Zizers, Switzerland) until the wire became red hot. This procedure was completed between inoculation of different isolates and when finished. All handling of live fungal isolates were done in biosafety cabinet for personal and environmental protection from fungal spores.

Cultivation for morphological identification was done by inoculation of fungal isolates on MEA and ½ PDA and incubated at 20 °C for 7 days. Observations of macromorphological features such as colony texture, form, size, adverse and reverse color and any production of exudate and / or pigments was recorded. The “Key to the common food- and indoor asexual genera” from Samson *et al.* (2019) was used as guide for identification at genus level (35).

2.3.2 Microscopy

Microscopy was used to identify micromorphological features such as hyphae, spore forming structures and spores. The adhesive tape preparation technique was used for microscopic examination. A droplet of lactofuchsin stain was applied to a microscopy slide and some drops of 70 % ethanol to a second slide. A folded strip of transparent adhesive tape was gently touched to the colony at the sporulating area. The tape was then gently washed in 70 % ethanol and the adhesive side of the tape was pressed to the slide with lactofuchsin. The prepared slide was inspected at 20x, 40x and 100x magnification using an eclipse N*i* (Nikon, Tokyo, Japan) microscope. Images were taken by the eclipse N*i* using a DS-Ri2 microscope camera (Nikon, Tokyo, Japan) with the NIS-Elements software platform (Nikon, Tokyo,

Japan). The stereo microscope SMZ1270 (Nikon, Tokyo, Japan) was also used for examination of the micromorphological structures.

2.3.3 Growth rate experiment

Potential LDPE degrading fungi were selected based on growth rate. Two growth rate tests were done on pure isolates, the first at 25 ± 1 °C and second at 20 ± 1 °C. A hemocytometer (Bürker counting-chamber) was used to adjust to a spore concentration of $1x10^6$ spores mL^{-1}. 100 µL of the spore concentration was applied in the center of 9 cm ∅ petri dish with ½ PDA. For the first and second experiment the samples were incubated at 25 ± 1 °C for 7 days and 20 ± 1 °C for 14 days, respectively. The minimum and maximum colony diameter was measured once a day for calculation of the mean colony diameter per day. The 11 fungal isolates with the highest growth rate at 20 °C were selected for further LDPE degrading analysis.

2.4 Molecular identification of fungal isolates

Molecular identification was done by characterization of the fungal genetic markers ITS and *tef1*.

2.4.1 DNA isolation

DNA isolation was done with QIAamp® DNA Mini QIAcube® Kit (QIAGEN, Hilden, Germany). Fungal mycelia and spores were collected with a pre-wet (with AL-buffer) cotton swab and added to a 2 mL micro-centrifuge tube containing 450 µL AL-buffer and a 4 mm stainless steel bead. Lysis and homogenization were performed using a MM 400 Mixer Mill (RETSCH, Haan, Germany) for 3 min at 25 Hz, followed by freezing at -80 ± 1 °C for 10 min and shock thaw and incubation at 56 ± 0.5 °C for 10 min. 10 µL of 20 mg mL^{-1} proteinase K solution were applied and incubated at 56 ± 0.5 °C for 30 min with shacking at 550 rpm. Samples were then centrifuged at 12 000 *g* for 5 min. After centrifugation 300 µL of the supernatant was further isolated and purified using the QIAcube® Connect (QIAGEN, Hilden, Germany) automated system with the QIAamp® DNA Mini Kit (QIAGEN, Hilden, Germany) procedure.

For every round of extraction, a contamination control named extraction blank control (EBK) was constructed by leaving a micro-centrifuge tube with lid open under the whole sample collection. The EBK was then extracted as a normal sample with 350 µL AL-buffer, 200 µL nuclease free water and a 4 mm stainless steel bead applied to a 2 mL micro-centrifuge tube.

Quantification and quality control of isolated DNA was verified using NanoDrop™ One Microvolume UV-Vis Spectrophotometer (Thermo Scientific™, Massachusetts, USA).

2.4.2 PCR and sequencing

Isolated DNA from each fungal strain was PCR amplified using nested primers for genetic marker loci as detailed in Table 3.

Table 3. Primers used for species identification. F and R in parenthesis are forward and revers primers, respectively. All primers were supplied by Invitrogen (Invitrogen, Carlsbad, USA).

Loci	Primers	Sequence 5' - 3'	Reference
ITS	ITS1 (F) ITS4 (R)	TCCGTAGGTGAACCTGCGG TCCTCCGCTTATTGATATGC	White *et al.* (1990) (59)
tef1	EF1 (F) EF2 (R)	ATGGGTAAGGARGACAAGAC GGARGTACCAGTSATCATGTT	O'Donnell *et al.* (1998) (60)
	EF1-728F (F) EF1-986R (R)	CATCGAGAAGTTCGAGAAGG TACTTGAAGGAACCCTTACC	Carbone *et al.* (1999) (61)

End-point PCR amplification of ITS and *tef1* loci was performed with illustra™ puReTaq Ready-To-Go™ PCR Beads (Cytivia, Massachusetts, USA) using a final primer concentration of 200 nM for each primer and 6.0 – 19.2 ng DNA template. One reaction of one genetic marker was constructed by applying 1 µL of each primer (forward and reverse), 21 µL of nuclease-free water and 2 µL of DNA template to the puReTaq Ready-To-Go PCR Bead, with a total volume of 25 µL, as described in Table 4. A "no template control" (NTC) sample using nuclease-free water instead of DNA template was added as a negative control. The PCR was conducted on the Veriti™ 96-Well Fast Thermal Cycler (Applied Biosystems, Massachusetts, USA) with the respective program as described in Table 5.

Table 4. PCR mastermix for the DNA amplification. Each PCR run had 11 samples, one EBK and one NTC. The nuclease-free water and primers were pooled together forming a master mix before adding 23 µL to each well, and then adding 2 µL of DNA template. 2 µL of nuclease-free water were added to the NTC. To compensate for pipetting errors one extra reaction was added.

Component	Volume 1rxn. (µL)	Volume 11+3rxn. (µL)	Final Concentration
puReTaq Ready-To-Go PCR Beads	-	-	1x
Forward primers (5 µM)	1.00	14.00	200 nM
Reverse primers (5 µM)	1.00	14.00	200 nM
Nuclease-free water	21.00	294.00	-
DNA template (2 - 8 ng / µL)	2.00	-	4 - 16 ng
Final Volume	**25.00**	**-**	**-**

Table 5. PCR program for the respective primers. The annealing temperature for the three primer pairs ITS1 + ITS4, EF1-728F + EF1-986R and EF1 + EF2 are 55 °C, 55 °C and 56 °C, respectively.

	ITS1 + ITS4		EF1-728F + EF1-986R		EF1 + EF2		
PCR program	**Temperature**	**Time**	**Temperature**	**Time**	**Temperature**	**Time**	**Repetitions**
Pre-denaturation	95 °C	8 min	95 °C	8 min	95 °C	5 min	1
Denaturation	95 °C	30s	95 °C	15 s	95 °C	30 s	
Annealing	**55 °C**	30s	**55 °C**	20 s	**56 °C**	20 s	35
Extension	72 °C	1 min	72 °C	1 min	72 °C	30 s	
Final extension	72 °C	10 min	72 °C	5 min	72 °C	5 min	1
End	4 °C	∞	4 °C	∞	4 °C	∞	-

A final quality control step of the PCR amplicon was done by agarose gel electrophoresis. A 1 % w / v agarose gel was constructed by weighing 1 g of Agarose I™ (VWR Chemicals, Ohio, USA) powder to 100 mL of TBE (45 mM Tris-borate, 1 mM EDTA). The solution was brought to a boil by microwaving for approximately 1.5 min and cooled down before adding 10 µL 10 000X GelRed® Nucleic Acid Gel Stain (biotium, California, USA). The solution was poured in a casting tray with an appropriate comb. DNA samples were prepared for gel electrophoresis by adding 5 µL PCR amplicon to 1 µL 6X DNA Loading Dye (Thermo Scientific™, Massachusetts, USA), and then applied to the set agarose gel. As a molecular-weight size marker 6 µL of premade (according to manufactures protocol) GeneRuler™ 1 kb DNA Ladder (Thermo Scientific™, Massachusetts, USA) was applied on both ends of the well lane on the agarose gel. The gel electrophoresis was run at 90 V for 45 min. Gel visualization was performed with Azure™ c150 Gel Imaging Workstation (Azure Biosystems, California, USA).

Sequencing was performed by Eurofins Genomics (Galten, Denmark) through the TubeSeq Service (Sanger sequencing). Eurofins Genomics received minimum 15 µl, recommended 10 ng μl^{-1} unpurified PCR amplicons from each isolate, which were purified through the additional service “DNA purification”. The primers ITS1 + ITS4 and EF1 + EF2 were used for sequencing with a primer concentration of 10 pmol μl^{-1}. Each primer had a minimum volume of 15 µl with additional 5 µl for every sequencing reaction.

2.5 Main experiment

The main experiment consisted of isolates from the collected soil samples and isolates from the strain collection (*Mykoteket*) of the Norwegian Veterinary Institute. With exception of VI 06793 (*Trichoderma trixiae*) the selection of fungal species / isolates from *Mykoteket* was based on publications, reporting these species to be capable of degrading PE plastics (28-31). VI 06793 (*T. trixiae*) was selected to gain more training and experience within the genus *Trichoderma*. Each isolate was cultured in six groups: two types of media and three time periods.

The primary screening for LDPE degradation capabilities was carried out in two series of media in triplicate. A 300 mL Erlenmeyer flask with 100 mL 2 % w / v glucose Mineral Salt Media (MSM, see Appendix 6.1 Culture Media) was inoculated with a fungal strain and a mean of 66 mg mixed LDPE TOs to identify any strains capable of glucose-assisted degradation of LDPE. The second series of strains and LDPE was inoculated in 100 mL glucose-free MSM, to identify any strains capable of utilizing LDPE as sole carbon source. Each flask was inoculated with 100 µL of pure isolates at a 1 x 10^6 mL^{-1} spore concentration quantified by hemocytometer. The Erlenmeyer flasks were loosely capped with sterile aluminum foil.

Each isolate triplet was assigned to a time period. Due to the slow growing nature of mesophilic fungi, the inoculum was incubated for 30, 60 and 90 days. Each media / time period group had two controls following the setup described in Table 6. For an overview of the study design see Figure 13.

Table 6. Overview of the different controls used in the primary screening.

Controls	Abbreviation	MSM	Glucose	Fungal inoculum	LDPE
Negative control 1	NC1	Yes	No	No	Yes
Negative control 2	NC2	Yes	No	Yes	No
Negative control 3	NC3	Yes	Yes	No	Yes
Positive control 1	PC1	Yes	Yes	Yes	No

The purpose of controls was to verify the study results or to trouble-shoot should it be necessary. Like the test samples, MSM was used in the controls. No growth was expected in the negative controls NC1, NC2 and NC3. The controls NC3 and NC1 were constructed for detecting changes in the LDPE TOs due to the MSM (with or without glucose), where NC3 also operates as a biological contamination control. NC2 contained fungal inoculum, but no carbon source, and therefore no growth. The positive control (PC1) had glucose, fungal inoculum and is expected to show growth. *Trichoderma harzianum* (VI 04074) was used in the PC1 as fungal inoculum and was selected based of rapid growth and as a well-studied species. If there was growth in the positive control, any absence of growth in the experimental flasks might be understood as not due to errors in laboratory work.

Isolates and controls were incubated at 20 ± 1 °C in a static condition for a duration of 0, 30, 60 and 90 days. After each of the respective 30 days intervals fungal mycelia were collected for determination of total biomass. LDPE TOs were collected and prepared for characterization of degradation by weight loss, ATR-FTIR and SEM.

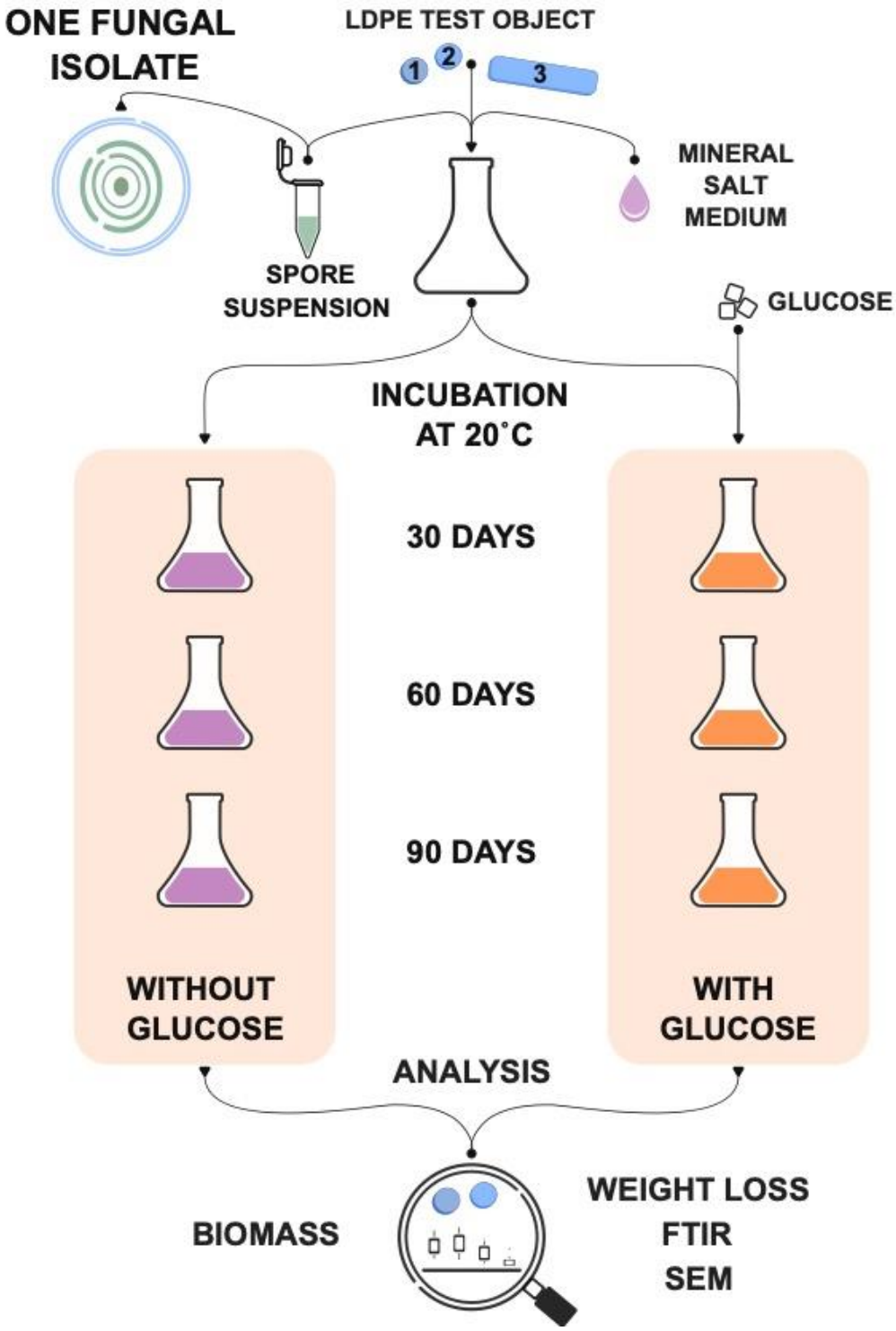

Figure 13. Schematic of the main experiment. The experiment consisted of isolates from the collected soil samples and isolates from the strain collection at the Norwegian Veterinary Institute, Mykoteket. Each isolate was grown with 100 mL MSM, a mean of 66 mg of LDPE TOs and 100 µL 1 x 10^6 spores mL^{-1} of pure isolate in a 300 mL Erlenmeyer flask. Three of the flasks were incubated without glucose and the other three with 2 % w / v glucose. These were statically incubated in total darkness at 20 ± 1 °C for 30, 60, and 90 days. This adds up to a total of 6 flasks per fungal isolate. LDPE TOs were analyzed for potential weight loss, changes in chemical functional groups by ATR-FTIR and changes on the surface by SEM. Lyophilized fungal biomass was also measured.

2.6 Measurement of fungal biomass

After the respective incubation intervals of 0, 30, 60 and 90 days fungal mycelia was filtered individually by vacuum filtration with the following setup from Millipore® (Merck, Darmstadt, Germany): 1.2 µm pore size glass fiber prefilter and 100 mL Microfil® funnel on the Microfil® filtration system with the EZ-Stream™ Vacuum pump. The LDPE TOs were picked out from the mycelium before freezing of prefilters at -80 ± 1 °C for a minimum of 12 hours. Frozen prefilters with fungal mycelium were transferred directly to the Freeze-drying system (BIOBASE, Shandong, China) for 48 hours of lyophilization. Measurement of dry biomass was done on a XPR105 Analytical Balance (Mettler Toledo, Greifensee, Switzerland) with five digits. A series of clean prefilters were vacuum filtered with MSM and freeze-dried with the other samples. After the lyophilization the mean weight of clean prefilters was subtracted from each dry mycelium weight.

2.7 Weight loss of Low-Density Polyethylene Test Objects

The LDPE TOs were extracted from the mycelium after the vacuum filtration following the respective incubation intervals of 0, 30, 60 and 90 days. Test objects from the 30 days incubation were transferred to microcentrifuge tubes and cleaned with distilled water and manually shaken by hand for a proximally 10 seconds. The microcentrifuge tubes were then centrifuged at 12 000 *g* for 5 min to sediment mycelial debris, followed by transfer of the test objects to new clean microcentrifuge tubes. LDPE TOs from the 60 days incubation were transferred to microcentrifuge tubes, then filled with distilled water and cleaned by ultrasonication on the 3510 Ultrasonic Cleaner (Branson Ultrasonics, Connecticut, USA) at 40 Hz for 60 min. After ultrasonication the microcentrifuge tubes were centrifuged at 12 000 *g* for 5 min to sediment mycelial debris, followed by transfer of the test objects to new clean microcentrifuge tubes. LDPE TOs from the 90 days incubation were cleaned with the same procedure as the 60 days LDPE TOs using ultrasonication. Additionally, LDPE TOs from the 90 days incubation were incubated at 25 ± 1 °C with 550 rpm for 4 hours. Independent of the incubation interval the LDPE TOs were air dried at room temperature (23 ± 2 °C) for 7 days and weighed on a XPR105 Analytical Balance (Mettler Toledo, Greifensee, Switzerland) with five digits. A weight control group for each respective test object type at day zero was calculated from the average weight of 58 LDPE TOs 1, 41 LDPE TOs 2 and 41 LDPE TOs 3.

Percentage weight loss was calculated using the formula given in Equation 1.:

Equation 1.

$$\frac{(LDPE\ test\ object\ weight - \bar{x}\ of\ control\ group)}{LDPE\ test\ object\ weight} * 100$$

LDPE TOs were stored in microcentrifuge tubes until further analysis by ATR-FTIR or SEM.

2.8 Attenuated Total Reflection Fourier Transform Infrared spectroscopy analysis

LDPE TOs from the primary screening were analyzed for potential oxidation using Attenuated Total Reflection Fourier Transform Infrared (ATR-FTIR) spectroscopy analysis.

Accelerated oxidation samples (positive controls) were constructed by incubating LDPE TOs at 95 ± 3 °C for 72 hours (3 days) and 168 hours (7 days).

The infrared spectra were collected using a Nicolet™ iS™ 5 FTIR Spectrometer with accessory iD7 ATR and processed by the OMNIC™ Software (Thermo Fisher Scientific, Massachusetts, USA). Spectra were collected in the region between 4000 and 400 cm^{-1} with 32 co-added scans. Background collections were done before every LDPE TO. The spectral resolution was 4 cm^{-1}. Every sample was analyzed in triplicates i.e., one of each LDPE TO type. Three untreated LDPE TOs were analyzed on each new day of analyzing true samples to ensure consistent results.

2.9 Scanning electron microscopy analysis

Potential changes in surface topography of the LDPE TOs were investigated using scanning electron microscopy (SEM). After the respective incubation interval of 0, 30, 60, and 90 days at least one LDPE TO of each type was transferred to microcentrifuge tubes and prepared for SEM. Fixation was done at 4 ± 1 °C for 12 hours in a fixative (see Appendix 6.1 Culture media) consisting of 2 % Paraformaldehyde and 1.25 % Glutaraldehyde in MSM (pH 6.5). The fixation liquid was then replaced with MSM, and samples were stored at 4 ± 1 °C until further sample preparation.

LDPE TOs were transferred with forceps to 7 mL Drams glasses containing 30 % ethanol and incubated for 10 minutes with shaking. The samples were then dehydrated through a graded ethanol series by replacing the ethanol with gradually increasing ethanol concentrations: 50 %, 70 %, 90 %, 96 %, finishing off with absolute ethanol (100 %) for a total of 4 times. Every step was incubated for 10 minutes with shaking. The dehydrated LDPE TOs were then transferred to the critical point dryer CPD 030 (BalTec, Pfäffikon, Switzerland). The ethanol was replaced with liquid CO_2, gently heated, and vented out. Samples were then placed on stubs with carbon tape and sputter coated twice with an 80 % gold and 20 % palladium mix for 80 seconds by a Range SC7640 Sputter Coater (Polaron, N / A, N / A). Samples were examined with the EVO®50 scanning electron microscope (Zeiss, Stuttgart, Germany) through the second electron detector.

2.10 Bioinformatic and statistical analysis

Raw sequencing reads from Eurofins were processed with the sequence analysis software Geneious Prime® v. 2022.0.1 (Biomatters, New Zealand). This includes manual inspection of sequence chromatograms, trimming of ends and global alignment of forward and reverse reads.

Statistical analysis of raw spectra from the ATR-FTIR analysis were done with The Unscrambler 11 (now Aspen Unscrambler™, Aspentech, Massachusetts, USA) software. This includes manual inspection of every spectrum, trimming, baseline correction, averaging of triplicates and Principal Component Analysis (PCA).

Collection of raw data of LDPE TO weight loss and fungal biomass were done in Microsoft® Excel for Mac v. 16.57 (Microsoft Corporation, Washington, USA).

ANOVA and *t-tests* as well as all plots were made with RStudio v. 1.4.1103 (RStudio Team, Massachusetts, USA). RStudio was also used for taxonomic identification by fungal ITS and *tef1* sequence analysis. The ITS sequences were used for genera identification by Basic Local Alignment Search Tool (BLAST) against the RefSeq ITS ftp-server (date: 28.02.22) (62). A self-prepared library of the gene *tef1* from *Trichoderma* spp. (date: 28.02.22) was used for the *tef1* sequence BLAST search. The ITS ftp-server and data for the *tef1* self-prepared library are available from NCBI (RefSeq ITS / Genebank – *tef1*).

Figures and some plots (from RStudio) were made / modified by the free and open-source vector graphics editor Inkscape v. 1.1.1 (c3084ef, 2021-09-22).

3 Results

3.1 Characterization of fungi results

A total of 37 fungal isolates were isolated from the soil samples (Table 7). From the private silage bale polywrap waste site 1, polywrap waste site 2, Valdres intermunicipal renovation, Valdresflye, Bølstad recycling station and Paddetjern there were isolated 4, 2, 6, 4, 10 and 11 isolates for each location, respectively. The vast majority of these isolates were not used in the main experiment due to poor growth rate at 25 °C on ½ PDA. Some isolates were excluded because they were thought to be potentially pathogenic fungi, like *Aspergillus niger* and *Aspergillus flavus*. Only one isolate per species and origin was selected, and thus some isolates of the same species and origin were excluded. This resulted in only 21 isolates being used in the second growth rate experiment at 20 °C on ½ PDA. The 11 isolates with the highest growth rate were selected for further use in the main experiment (Figure 14). These were two isolates from polywrap waste site 1, one from polywrap waste site 2, two from Valdres intermunicipal renovation, one from Valdresflye, three from Bølstad recycling station and two from Paddetjern (Table 7).

Table 7. Overview of the different isolates cultivated from soil samples and of the fungal species from the strain collection Mykoteket. Fungal species from Mykoteket are all morphologically characterized. [a] Indicates that the isolate was excluded from further use in this study and was therefore not assigned an Isolate number nor sequenced for molecular identification. [b] This information has been omitted due to customer confidentiality conditions at the Norwegian Veterinary Institute. [c] VI 05132 (Aspergillus terreus) has not yet been confirmed with molecular identification. [d] Only one species call indicates agreement between the different molecular markers. See section 3.1.3 Molecular analysis for further explanation.

ID	Origin	Molecular marker	Species
Isolate 01	Polywrap waste site 1	ITS / *tef1*	*Trichoderma rifaii / Trichoderma atrobrunneum*
- [a]	Polywrap waste site 1	-	-
-	Polywrap waste site 1	-	-
Isolate 02	Polywrap waste site 1	ITS / *tef1*	*Trichoderma virilente / Trichoderma paraviridescens*
Isolate 03	Polywrap waste site 2	ITS / *tef1*	*Trichoderma inhamatum / Trichoderma harzianum*
-	Polywrap waste site 2	-	-
-	Valdres intermunicipal renovation	-	-
Isolate 04	Valdres intermunicipal renovation	ITS / *tef1*	*Trichoderma viride* [d]
-	Valdres intermunicipal renovation	-	-
Isolate 05	Valdres intermunicipal renovation	ITS / *tef1*	*Trichoderma virilente / Trichoderma paraviridescens*
-	Valdres intermunicipal renovation	-	-
-	Valdres intermunicipal renovation	-	-
-	Valdresflye	-	-
Isolate 06	Valdresflye	ITS / *tef1*	*Trichoderma viridescens / Trichoderma paraviridescens*
-	Valdresflye	-	-
-	Valdresflye	-	-
-	Bølstad recycling station	-	-
-	Bølstad recycling station	-	-
-	Bølstad recycling station	-	-
Isolate 07	Bølstad recycling station	ITS / *tef1*	*Trichoderma ghanense / Hypocrea lixii*
Isolate 08	Bølstad recycling station	ITS / *tef1*	*Trichoderma inhamatum / Trichoderma ghanense*
-	Bølstad recycling station	-	-
-	Bølstad recycling station	-	-
Isolate 09	Bølstad recycling station	ITS / *tef1*	*Trichoderma asperellum*
-	Bølstad recycling station	-	-
-	Bølstad recycling station	-	-
-	Paddetjern	-	-
-	Paddetjern	-	-
-	Paddetjern	-	-
-	Paddetjern	-	-
-	Paddetjern	-	-
-	Paddetjern	-	-
-	Paddetjern	-	-
-	Paddetjern	-	-
-	Paddetjern	-	-
Isolate 10	Paddetjern	ITS / *tef1*	*Trichoderma hamatum*
Isolate 11	Paddetjern	ITS / *tef1*	*Trichoderma atroviride*
VI 06533	NA [b]	*tub2*	*Aspergillus sydowii*
VI 05132	NA	[c]	*Aspergillus terreus*
VI 06901	NA	*tub2*	*Penicillium chrysogenum*
VI 04074	NA	ITS	*Trichoderma harzianum*
VI 06793	NA	*tef1*	*Trichoderma trixiae*

Originally, 12 fungal species from the strain collection *Mykoteket* were chosen as positive controls for degradation of LDPE based on relevant publications. Two isolates of *Aspergillus flavus* were on the original list but were excluded from further use due to its known pathogenicity and toxicity. Due to capacity and logistical constraints, the final five species were shortlisted for further experiments (Table 7*)*.

3.1.1 Growth rate results

High growth rate at 20 °C (14 days on ½ PDA) was the sole selection criterium for further examination of fungal isolates, and thus 11 isolates were selected from the soil samples. The results of the growth rate test are presented in Figure 14. Most of the soil isolates covered the entire petri dish (9 cm ∅) on day 4 of incubation, with three exceptions. These three exceptions were Isolates 02, 06, and 09 which reached a mean colony diameter of 9 cm on day 6, 5 and 7, respectively. The growth rate test was done with the isolates from *Mykoteket* as well, and the two reference isolates *Trichoderma harzianum* (VI 04074) and *Trichoderma trixiae* (VI 06793) covered the petri dish on day 4 of incubation. The three species *Aspergillus terreus* (VI 05132), *Aspergillus sydowii* (VI 06533) and *Penicillium chrysogenum* (VI 06901) grew slower with a mean colony diameter of 7.3, 4.3 and 6 cm after 14 days of incubation, respectively.

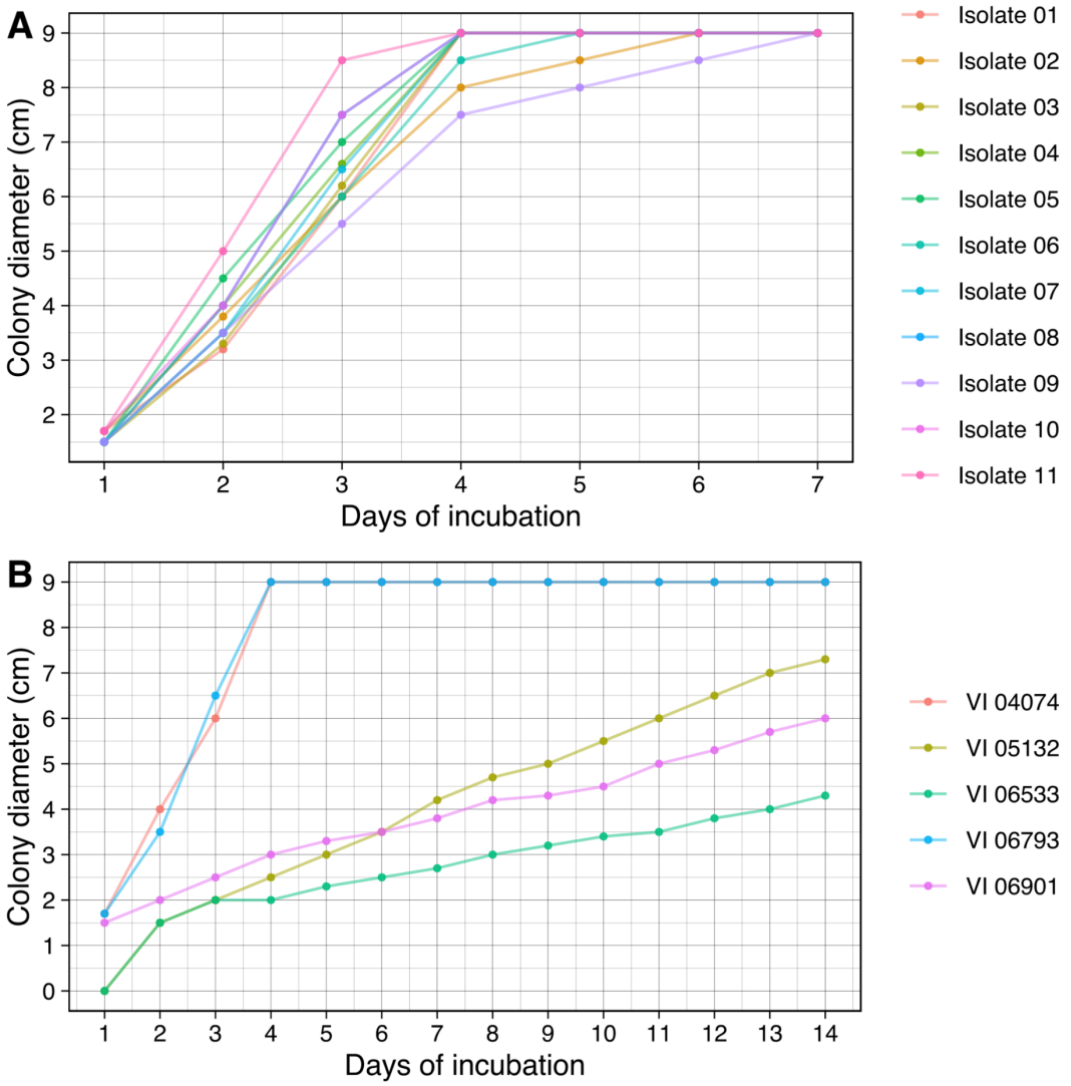

*Figure 14. Growth rate of fungal isolates from soil (**A**) and Mykoteket (**B**) incubated at 20 °C. Fungal isolates from soil covered the entire petri dish (∅ = 9 cm) within 7 days, where the majority reached it on day 4 (**A**). Isolate 02, Isolate 06, and Isolate 09 covered the petri dish on day 6, 5 and 7, respectively. Fungal reference isolates from Mykoteket (**B**). The two fungal species Trichoderma harzianum (VI 04074) and Trichoderma trixiae (VI 06793) covered the petri dish on day 4 of incubation. The other three species Aspergillus terreus (VI 05132), Aspergillus sydowii (VI 06533) and Penicillium chrysogenum (VI 06901), had a mean colony diameter of 7.3, 4.3 and 6 cm after 14 days of incubation.*

3.1.2 Morphological characteristics results

The macro- and micro-structures of the isolates were studied for morphological identification to the genus level of the isolates. General macromorphological features such as growth rate and colony coloration were recorded. Aggregates of conidiophores distributed in concentric circles from the center were also observed. Isolate 06 and 09 were the only ones with altered reverse color, which were yellow. Of micromorphological structures, highly branched main axis with phialides often bearing on conidia was observed. The conidia appeared as globose or ovoid. All the soil isolates showed general features of the genus *Trichoderma*. In Figure 15, the Isolates 01, 06 and the *Mykoteket* isolate VI 05132 are presented with colonies on petri dish, in test Erlenmeyer-flask, on filter disk and images from stereo microscope and light microscope, respectively.

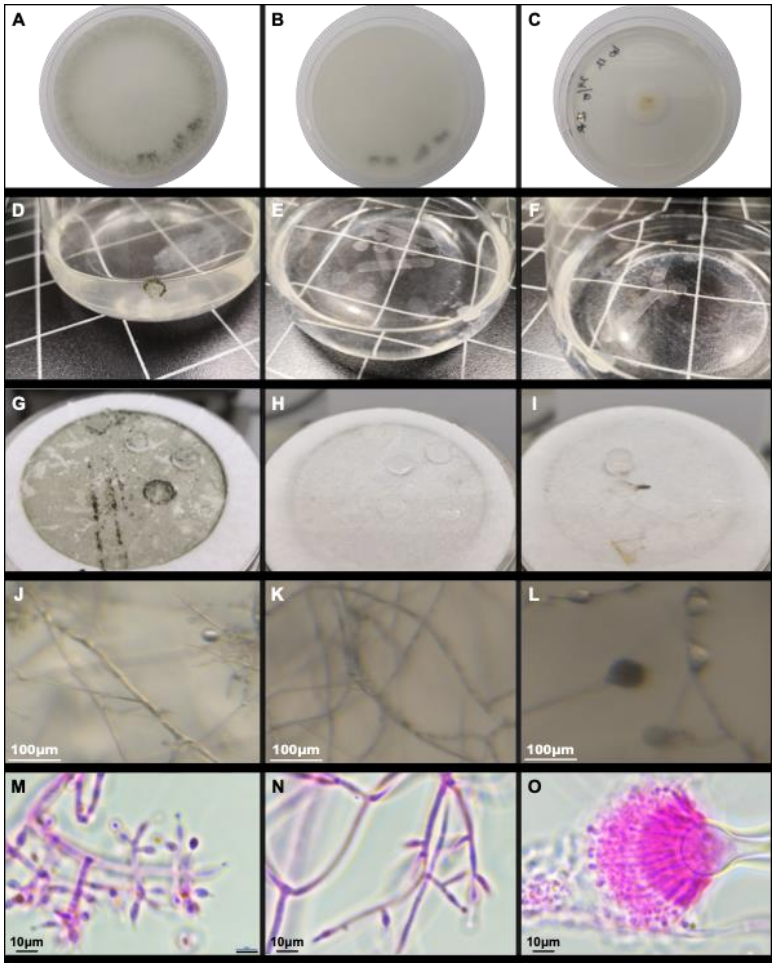

*Figure 15. Images of micro- and macromorphological structures of Isolate 01 (**A**, **D**, **G**, **J** and **M**), Isolate 06 (**B**, **E**, **H**, **K** and **N**) and Mykotek isolate VI 05132 (**C**, **F**, **I**, **L** and **O**) are presented by each its own column. (**A**, **B** and **C**) Fungal colonies observed on petri dishes, (**J**, **K** and **L**) images from stereo microscopes and (**M**, **N** and **O**) images from light microscopes are incubated on MEA at 20 °C for 7 days. LDPE TOs (**D**, **E** and **F**) before and (**G**, **H** and **I**) after vacuum filtration inoculated with given isolates incubated with MSM without glucose at 20 °C for 90 days.*

3.1.3 Molecular analysis results

The 11 isolates selected for further experiments were analyzed using ITS and *tef1* as genetic markers for molecular identification. The quality control of the PCR reaction was done with agarose gel electrophoresis, where the image indicates an average amplicon size between 500 bp – 750 bp for ITS amplified with primers ITS1 / ITS4 (Figure 16 – A). The primer combination EF1-728F / EF1-986R gave no amplification for *tef1* (result not shown), however primer pair EF1 / EF2 gave a PCR product of 750bp – 1000bp (Figure 16 – B). The sequencing was therefore done with primers ITS1 and ITS4 for the ITS marker and primers EF1 and EF2 for *tef1*.

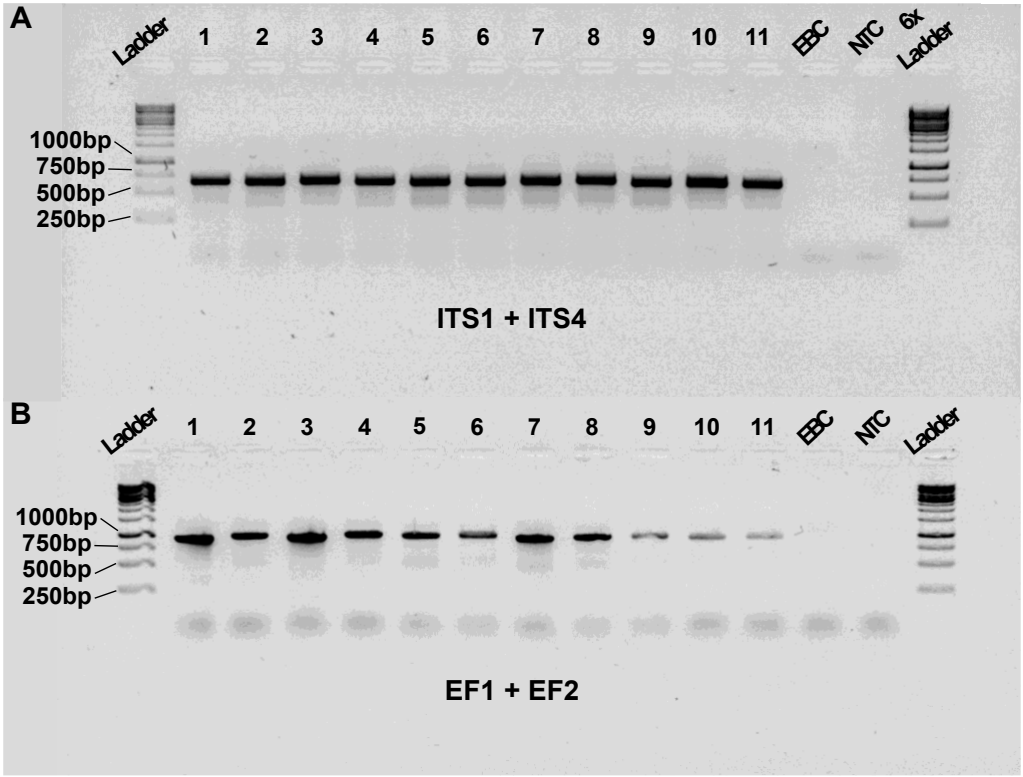

*Figure 16. Gel electrophoresis image of PCR amplicons of the genetic markers. The primer pairs used are the ITS1 / ITS4 for the ITS marker (**A**) and EF1 / EF2 for the tef1 marker (**B**). Based on the DNA ladder the approximate size of the amplicons are 500 bp – 750 bp and 750 bp – 1000 bp for the ITS and tef1, respectively. Ladder (molecular-weight size marker); Numbers indicate isolate number; EBC (extraction blank control); NTC (no template control). Fragments sizes of the DNA ladder (in base pairs) are marked 1000 bp, 750 bp, 500 bp and 250 bp. The image was inverted by the gel imaging software.*

The BLAST search of the ITS sequences showed highest similarity with the genus *Trichoderma* for all isolates, with an identity > 99 %. For the majority of the isolates BLAST search of the *tef1* sequence differed in species call compared to the ITS search, but the percent identity of *tef1* was in all cases greater than for ITS. There were four isolates where ITS and *tef1* species did correspond in species call: Isolate 04 – *Trichoderma viride*; Isolate 09 – *Trichoderma asperellum;* Isolate 10 – *Trichoderma hamatum;* Isolate 11 – *Trichoderma atroviride*. For a comprehensive best hit table of ITS and *tef1* BLAST search, see Table 8.

Table 8. Results of BLAST search for the genetic markers ITS and tef1 of the respective soil isolates. The percent identity (% Identity) is the similarity of the query sequence (Isolate 01 – 11) against a reference sequence in the data base. Percent identity gives therefore the percent identical nucleotides between the two aligned sequences. The table shows only the best hit filtered by "% Identity" for the respective marker.

Isolate	**% Identity ITS**	**Species ITS**	**% Identity *tef1***	**Species *tef1***
Isolate 01	99.8	*Trichoderma rifaii*	100	*Trichoderma atrobrunneum*
Isolate 02	100	*Trichoderma virilente*	100	*Trichoderma paraviridescens*
Isolate 03	99.6	*Trichoderma inhamatum*	100	*Trichoderma harzianum*
Isolate 04	100	*Trichoderma viride*	99.8	*Trichoderma viride*
Isolate 05	100	*Trichoderma virilente*	100	*Trichoderma paraviridescens*
Isolate 06	100	*Trichoderma viridescens*	100	*Trichoderma paraviridescens*
Isolate 07	99.6	*Trichoderma ghanense*	100	*Hypocrea lixii*
Isolate 08	99.1	*Trichoderma inhamatum*	99.4	*Trichoderma ghanense*
Isolate 09	99.8	*Trichoderma asperellum*	100	*Trichoderma asperellum*
Isolate 10	100	*Trichoderma hamatum*	100	*Trichoderma hamatum*
Isolate 11	99.8	*Trichoderma atroviride*	100	*Trichoderma atroviride*

Isolate 02 and 05 are the only isolates that have the same species call at both ITS and *tef1* gene marker, *Trichoderma virilente* and *Trichoderma paraviridescens*, respectively. Both isolates are cultivated from soil samples from Valdres. Isolate 02 originates from polywrap waste site 1 and Isolate 05 originates from Valdres intermunicipal renovation.

3.2 Measurements of fungal freeze-dried biomass results

The use of LDPE as carbon source is associated with gain of biomass. Measurements of freeze-dried mycelia can therefore be indirectly indicative of LDPE degradation. Normalized freeze-dried mycelial weights are presented in Figure 17. There is a clear trend whether glucose is present or not. This is supported by *t-test's* where it was found a significant difference between presence or absence of glucose every incubation interval with a *p-value* < 0.001. There was not found any statistical significance between the three incubation periods incubated without glucose for 30, 60 and 90 days. It was, however, found a statistically significant difference between 60 and 90 days of incubation with glucose (*p-value* < 0.05).

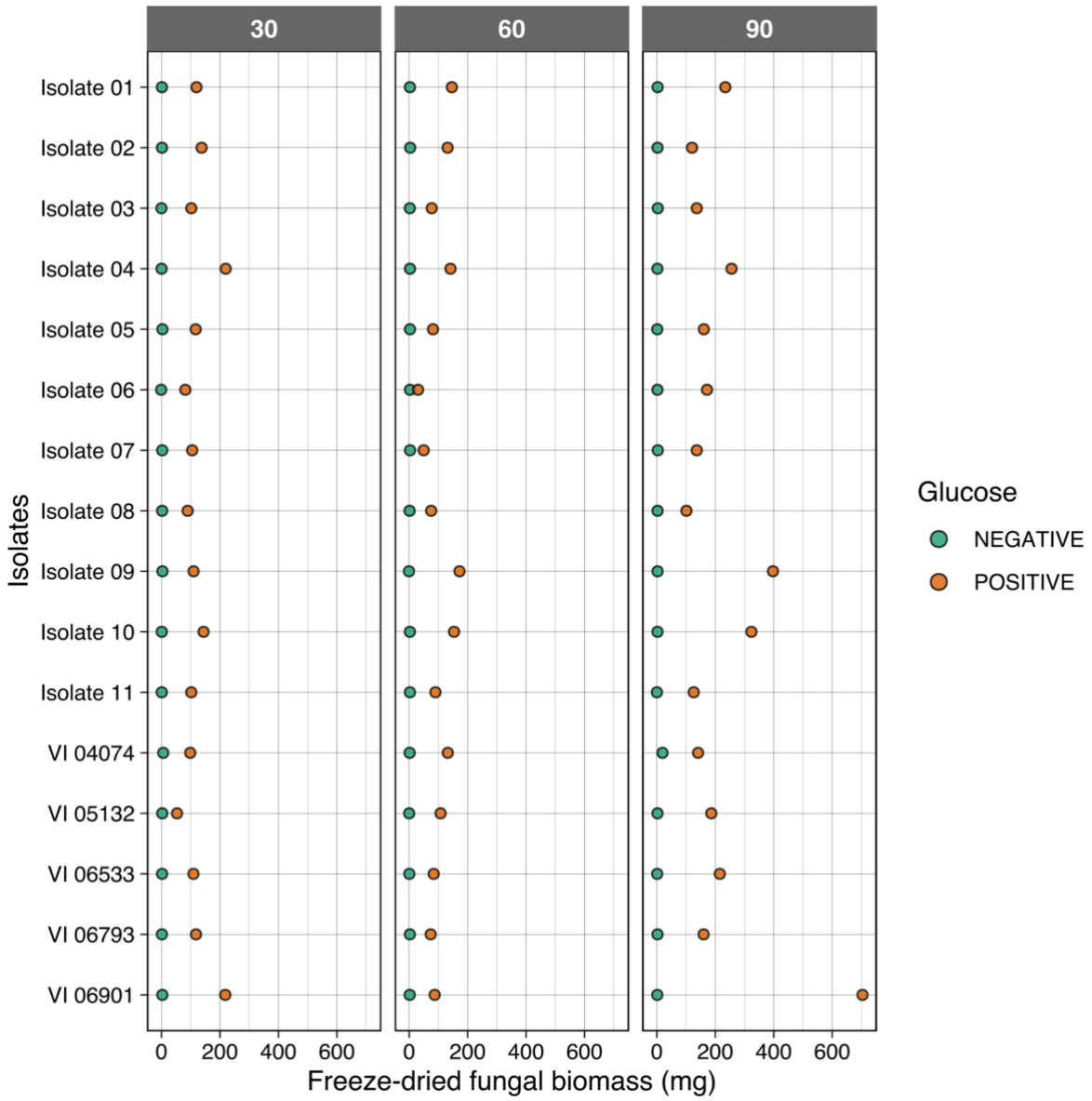

Figure 17. Freeze-dried fungal biomass (mg) of the different isolates grown with and without glucose for 30, 60 and 90 days (n = 6 per isolate).

None of the individual isolates shows any tendency to gain significant biomass independent of the presence of glucose. There are two extreme observations that are potential outliers according to the interquartile rage criterion (outlier = $[Q_{0.25} - 1.5 \cdot IQR; Q_{0.75} + 1.5 \cdot IQR]$). These are VI 04074 (*Trichoderma harzianum*) without glucose and VI 06901 (*Penicillium chrysogenum*) with glucose incubated for 90 days with a freeze-dried biomass of 19.23 mg and 703.54 mg, respectively (Table 9).

Table 9. Descriptive statistics of freeze-dried fungal biomass (mg). Values are for the groups with or without glucose incubated at 30, 60 or 90 days (n = 16). Difference is the maximum value subtracted by the minimum value.

Glucose	Incubation (days)	Minimum (mg)	Mean (mg)	Median (mg)	Maximum (mg)	Difference (mg)
NEGATIVE	30	-1.05	1.87	1.87	5.88	6.93
	60	-0.85	1.88	2.33	3.25	4.10
	90	0.12	3.19	2.29	19.23	19.11
POSITIVE	30	53.18	120.25	109.51	219.68	166.50
	60	30.42	101.98	88.48	172.18	141.76
	90	101.22	223.15	166.20	703.54	602.32

Growth was measured in all controls at different incubation periods as freeze-dried mycelium (results not shown). Growth in the controls NC1 and NC2 was measured as 10.51 mg and 15.06 mg, respectively, both of which were incubated without glucose for 90 days. The NC1 contained LDPE TOs, but no fungal inoculum incubated for 30, 60 and 90 days. Where NC2 were inoculated for 30, 60 and 90 days with *T. harzianum*, but did not contain LDPE TOs. Growth was also measured in NC3 at 60 days of incubation as 62.43 mg and 90 days of incubation as 72.77 mg. NC3 was incubated with glucose and LDPE TOs for 30, 60 and 90 days, but without fungal inoculum. Growth was recorded in PC1 to be 61.92 mg, 62.43 mg and 32.66 mg of freeze-dried biomass for the three timepoints. PC1 contained glucose and inoculum of *T. harzianum,* but no TOs.

3.3 Weight loss of Low-Density Polyethylene Test Objects results

One of the methods used to determine plastic utilization as carbon source is the relative weight loss of the plastic specimen. With the study design used, this generated six flasks per isolate, i.e., two flasks (with or without the presence of glucose) for every incubation interval 30, 60 and 90 days. An average of 66 mg of LDPE TOs was added to each isolate / glucose / incubation.

A *t-test* was performed on the absolute weight (mg) between the two groups with or without glucose at every incubation interval. These *t-tests* showed no statistical difference between the groups with or without glucose within the respective incubation interval. The lack of trend between with or without glucose is presented in Figure 18.

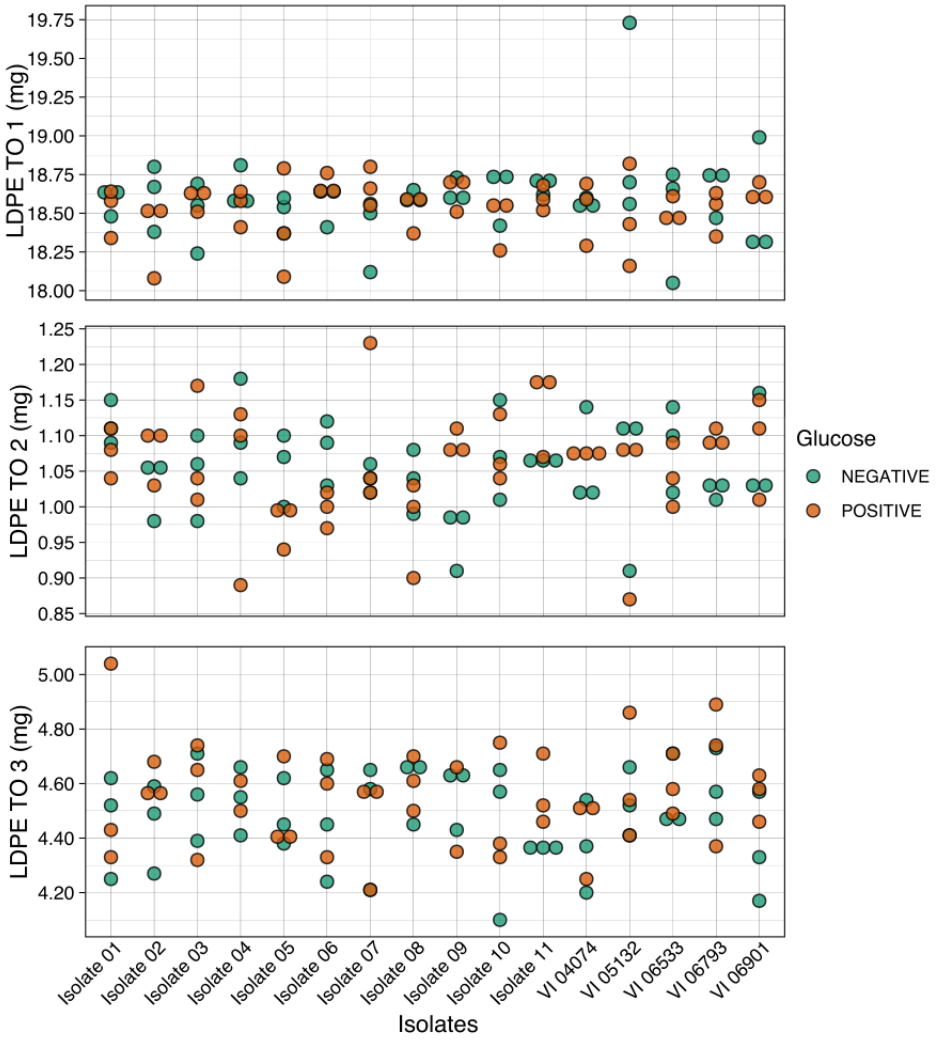

Figure 18. Distribution of LDPE TO weight (mg) for the different isolates. For every isolate there are one dot for incubation with or without glucose at the three timepoints 30, 60 and 90 days (n = 6 per isolate per timepoint). The dots are not grouped by incubation interval at any means. The first (top) plot shows the weight for LDPE TO 1, the second is the LDPE TO 2 and the third (bottom) shows the weight of LDPE TO 3. The orange (positive) and green (negative) dots indicates incubation with and without glucose, respectively.

Therefore, the groups with and without glucose were pooled to make a greater sample size (n = 34) per incubation interval (two controls included). The control group (day zero) comprised of 58 LDPE TOs 1, 41 LDPE TOs 2 and 41 LDPE TOs 3. Statistical significance was determined by *t-tests* between the control group and the three incubation intervals. The compared means are presented in Table 10.

Table 10. Descriptive statistics for the measured weighs (mg) of the three types of LDPE TO. Values are for the pooled group of with and without glucose (n = 34) incubated at 30, 60 or 90 days. The control group is TOs from day zero (n = 58 for LDPE TO 1, and n = 41 for LDPE 2 and 3). Difference is the maximum value subtracted by the minimum value.

	Incubation (days)	**Minimum (mg)**	**Mean (mg)**	**Median (mg)**	**Maximum (mg)**	**Difference (mg)**
LDPE TO 1	Control	18.11	18.67	18.69	19.02	0.91
	30	18.09	18.60	18.62	19.73	1.64
	60	18.12	18.54	18.57	18.99	0.87
	90	18.05	18.57	18.58	18.82	0.77
LDPE TO 2	Control	0.88	1.08	1.08	1.25	0.37
	30	0.91	1.06	1.07	1.15	0.24
	60	0.87	1.03	1.03	1.23	0.36
	90	0.97	1.08	1.08	1.18	0.21
LDPE TO 3	Control	3.99	4.5	4.58	4.83	0.84
	30	4.25	4.49	4.46	4.74	0.49
	60	4.2	4.53	4.56	4.89	0.69
	90	4.1	4.56	4.57	5.04	0.94

For the LDPE TO 1 a statistically significant difference was found between the control group and 60 days of incubation with a *p-value* < 0.01. There was also found a significant difference between the control group and 90 days of incubation with a *p-value* < 0.05. There was not found any statistical significance between the control group and the three incubation intervals for neither LDPE TO 2, nor LDPE TO 3.

The two measurements mean, and median are typically used for observing central tendency. The mean is commonly used in the statistical testing but is not a robust statistic. In contrast to the mean, the median is not skewed by extreme values. Since these measures are relatively equal within the same group (Control, 30, 60 and 90), it is assumed that the distribution is not

notable skewed (Table 10). The weight distribution of LDPE TOs grouped by 0 (control), 30, 60 and 90 days of incubation are presented in Figure 19.

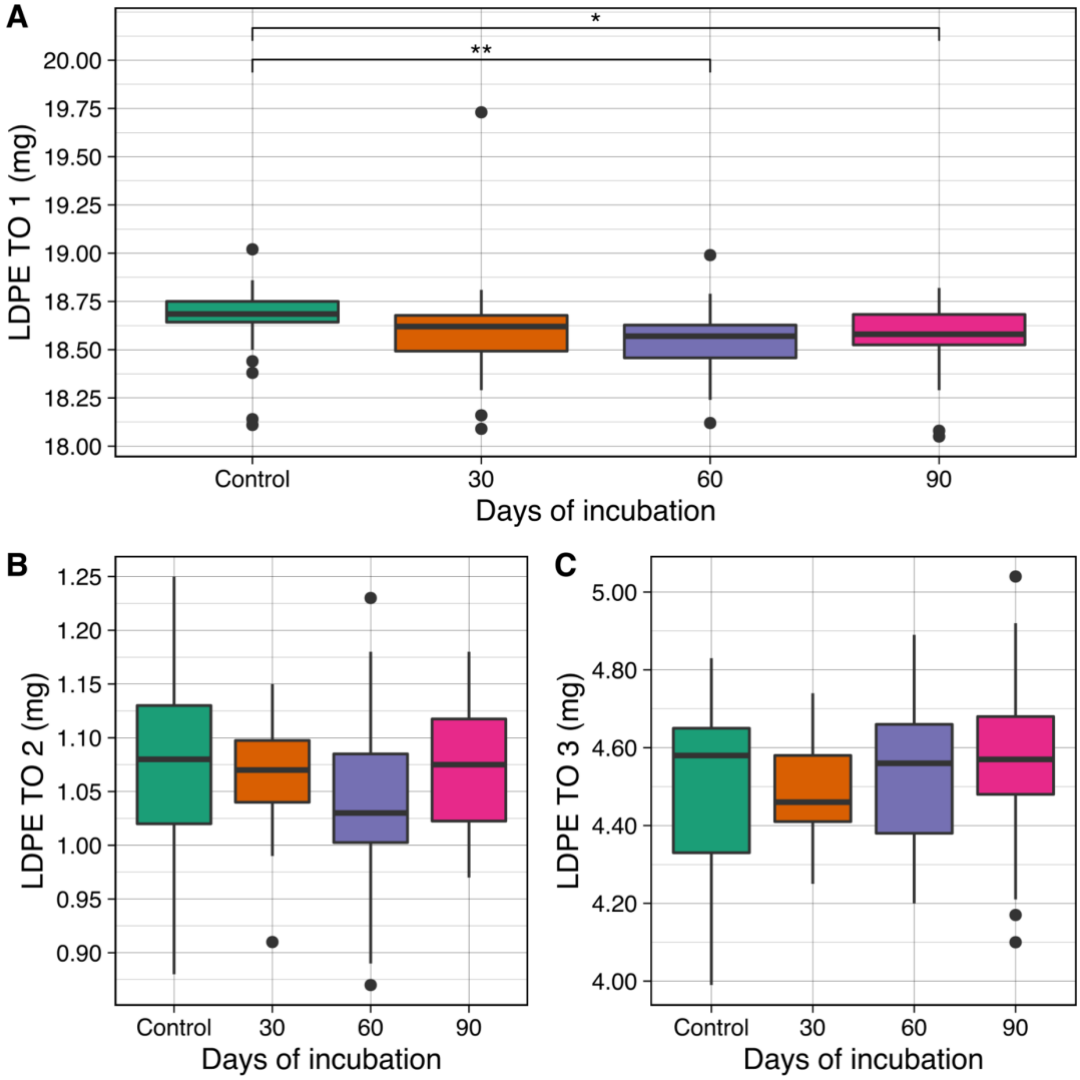

*Figure 19. Weight (mg) distribution of the three groups of LDPE TOs. Test objects from medium with and without glucose were pooled for each time point. This resulted in a sample size of 34 observations for the given incubation interval (NC1 and NC3 controls included). The control group comprised of 58, 41 and 41 test objects from LDPE TO 1, LDPE TO 2 and LDPE TO 3, respectively. The black horizontal line inside the box represents the median, the box represents the interquartile range (IQR, 50% of the observations) and outliers are represented by black dots. Boxplot of group 1 test objects (**A**). The asterisk (*) indicates a statistically significant difference between Control and 90 days, with a p-value < 0.05. The ** indicates a statistically significant difference between Control and 60 days, with a p-value < 0.01. Boxplot of LDPE TO 2 and 3 (**B** and **C**). No statistical significance was found between the control group and the three incubation intervals for LDPE TO 2 or 3.*

The distribution within the groups of the different LDPE TOs is relatively equal. The calculated differences (maximum value subtracted by the minimum value) are also relatively equal within the LDPE TOs and between the LDPE TOs (Table 10). This indicates the same natural variation across the groups and between LDPE TOs.

The relative weight loss of LDPE TO 1 is presented in Figure 20. The calculations were done according to Equation 1 (2.7 Weight loss of Low-Density Polyethylene Test Objects). The mean percentage weight loss across incubations were 0.2 % – 0.8 % (min. -5.6 % / max. 3.4 %) without glucose and 0.6 % – 0.8 % (min. -0.7 % / max. 3.2 %) with glucose (Table 11). A negative percentage weight loss indicates weight gain relative to the control group. There is no indication of glucose affecting the weight loss significantly. This applies within the isolates and incubation intervals. The same trend (or rather the lack of trend) applies to the other LDPE TOs as well (see Appendix 6.2.1 Weight loss of Low-Density Polyethylene Test Objects).

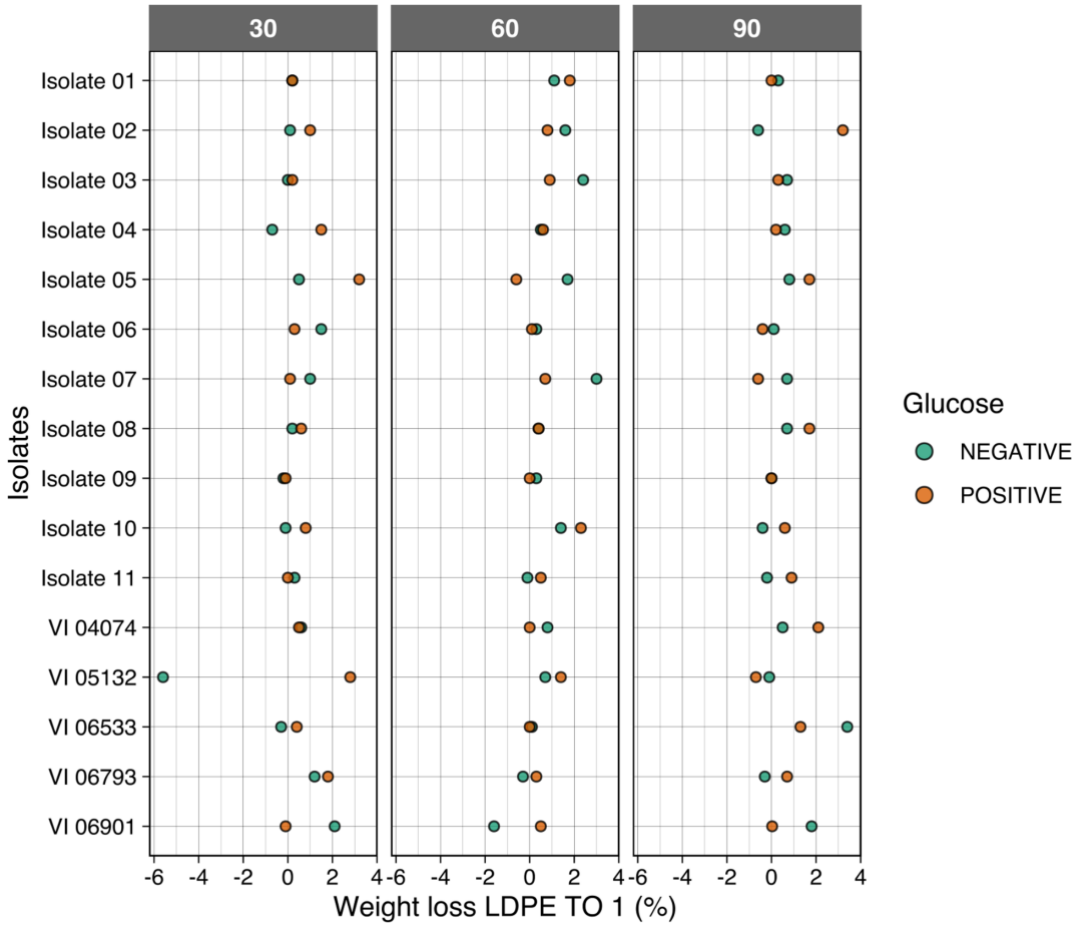

Figure 20. Weight loss in percentage for LDPE TO 1 (n = 6 with per isolate) through the three incubation periods 30, 60 and 90 days with (positive) or without (negative) glucose. The figure is representative of TO 2 and 3 as well (see Appendix 6.2.1 Weight loss of Low-Density Polyethylene Test Objects).

Table 11. List of descriptive statistics of relative (%) weight loss for LDPE TO 1 without (negative) and with (positive) the presence of glucose (n = 48). Difference is the maximum value subtracted by the minimum value.

Glucose	Incubation (days)	Minimum (%)	Mean (%)	Median (%)	Maximum (%)	Difference (%)
NEGATIVE	30	-5.6	0.2	0.2	2.1	7.7
	60	-1.6	0.8	0.7	3.0	4.6
	90	-0.6	0.5	0.3	3.4	4.0
POSITIVE	30	-0.1	0.8	0.4	3.2	3.3
	60	-0.6	0.6	0.5	2.3	2.9
	90	-0.7	0.7	0.6	3.2	3.9

3.4 Attenuated Total Reflection Fourier Transform Infrared spectroscopy results

ATR-FTIR spectroscopy was performed to assess potential utilization of LDPE by the fungal species at a chemical level. ATR-FTIR was applied to analyze for potential oxidization with the emphasis on the carbonyl (C = O) containing functional groups (e.g., aldehyde, ketone, carboxylic acid, ester, amide). Spectra were collected from one of every LDPE TO type from all isolates (and control NC1 and NC3) at each timepoint with / without glucose. A spectrum of LDPE TO 1 is presented in Figure 21 and originated from Isolate 01 incubated for 90 days without glucose. The figure shows the spectral ranges 3500 – 600 cm^{-1} and 1850 – 1420 cm^{-1}. The former is the full range spectrum, and the latter is the Carbonyl Index- (CI) and reference-region of the spectrum. From 3500 – 600 cm^{-1} this results in absorbance peaks at 2914, 2846, 1471, 1462, 1375, 729 and 718 cm^{-1}. The presented spectrum (Figure 21) is a representative for the total collected spectra (n = 306) with no peaks in the CI-region.

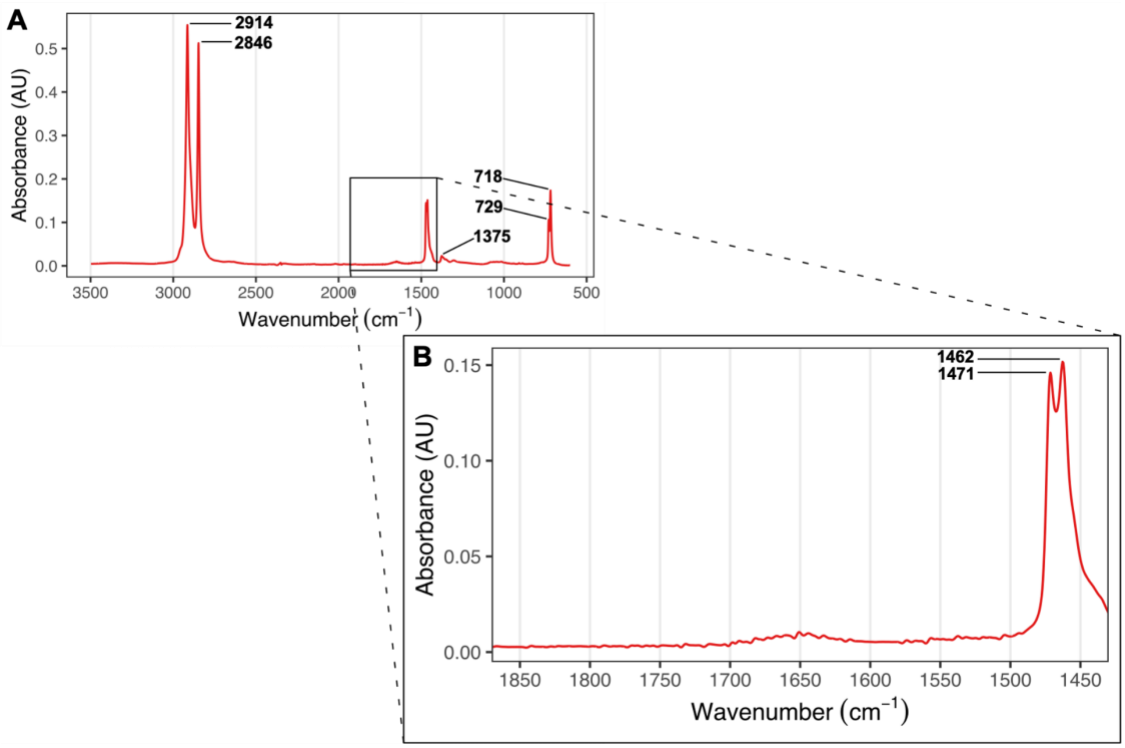

*Figure 21. ATR-FTIR spectra of LDPE TO 1 from Isolate 01, 90 days of incubation with no glucose. This spectrum is typical for how the other spectra also look like (n = 306). Full spectral range (3500 – 600 cm^{-1}) with the respective peaks; 2914, 2846, 1375, 729 and 718 cm^{-1}(**A**). Spectra of Carbonyl index region (1850 – 1650 cm^{-1}) and reference region (1500 – 1420 cm^{-1}) with the peaks 1471 and 1462 cm^{-1}(**B**).*

A positive oxidation control was constructed to demonstrate potential oxidation of the LDPE TOs and the following spectra after analyzing by ATR-FTIR. Spectra of untreated LDPE TO 1 and photo- and thermal treated (positive oxidation control) are shown in Figure 22. The photo- and thermal treated samples were exposed to UVC radiation for 24 hours and heat treated at 95 °C for 7 days. The untreated LDPE TO 1 spectrum had absorbance peaks at 2914, 2846, 1471, 1462, 1375, 729 and 718 cm^{-1}. The photo - and thermal treated LDPE TO 1 have the same peaks as the untreated, but with an additional peak at 1714 cm^{-1} within the CI-region 1850 – 1650 cm^{-1}. This peak indicates some oxidation of the LDPE TO 1. Other positive oxidation controls were constructed by UVC radiation for 24 hours and heat treated at 95 °C for 3 days instead of 7, but these showed no peaks within the CI-region (*results not shown*).

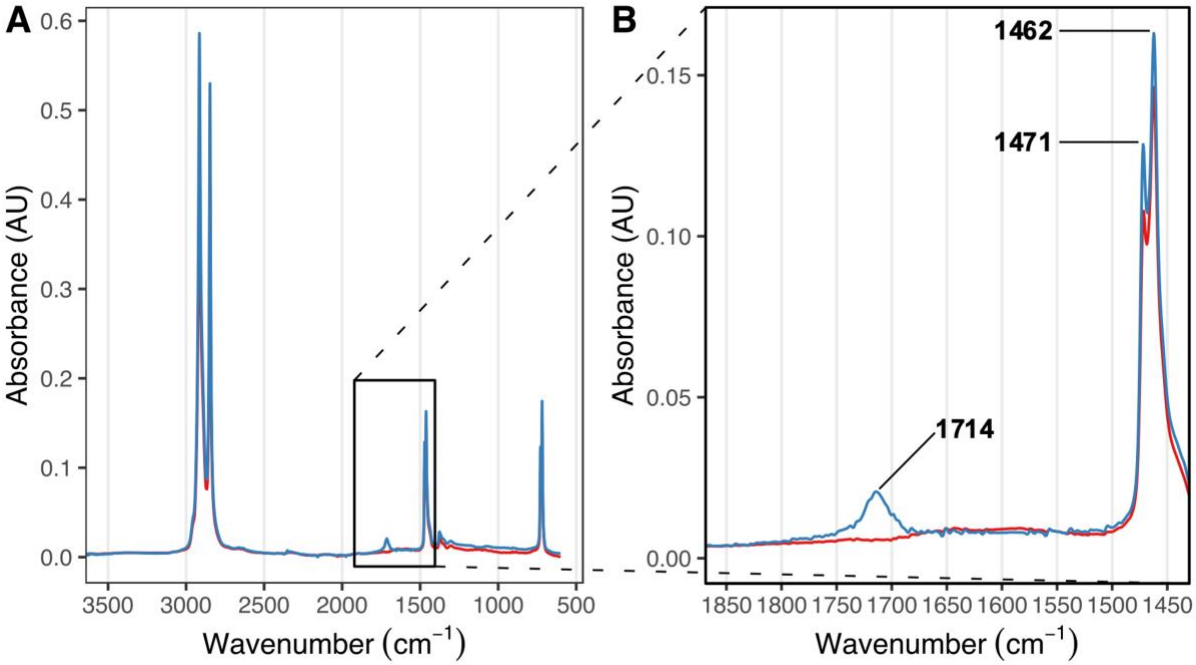

*Figure 22. ATR-FTIR spectra of LDPE TO 1 from untreated control (red) and photo- and thermal treated positive control (blue). The photo- and thermal treated sample was exposed to UVC radiation for 24 hours, and heat treated at 95°C for 7 days. Full spectral range (3500 – 600 cm^{-1}) with peaks at: 2914, 2846, 1714, 1375, 729 and 718 cm^{-1} independent of sample (**A**). Spectrum of Carbonyl index region (1850 – 1650 cm^{-1}) and reference region (1500 – 1420 cm^{-1}) (**B**). The photo- and thermal treated LDPE TO 1 (blue) has an additional peak at 1714 cm^{-1}. Both samples have peaks at 1471 and 1462 cm^{-1} in the reference region.*

There is a difference in chemical composition between LDPE TO 1 and LDPE TO 2 / 3 which in turn results in different spectra. Spectra of LDPE TO 1 and LDPE TO 2 from 0 days of incubation are presented in Figure 23. Test objects 1 and 2 had the same peaks at 2914, 2846, 1471, 1375, 729 and 718 cm^{-1}, whereas LDPE TO 1 had an additional peak at 1462 cm^{-1}, lacking in TO 2. LDPE TO 3 had the same peaks as LDPE TO 2 (*results not shown*).

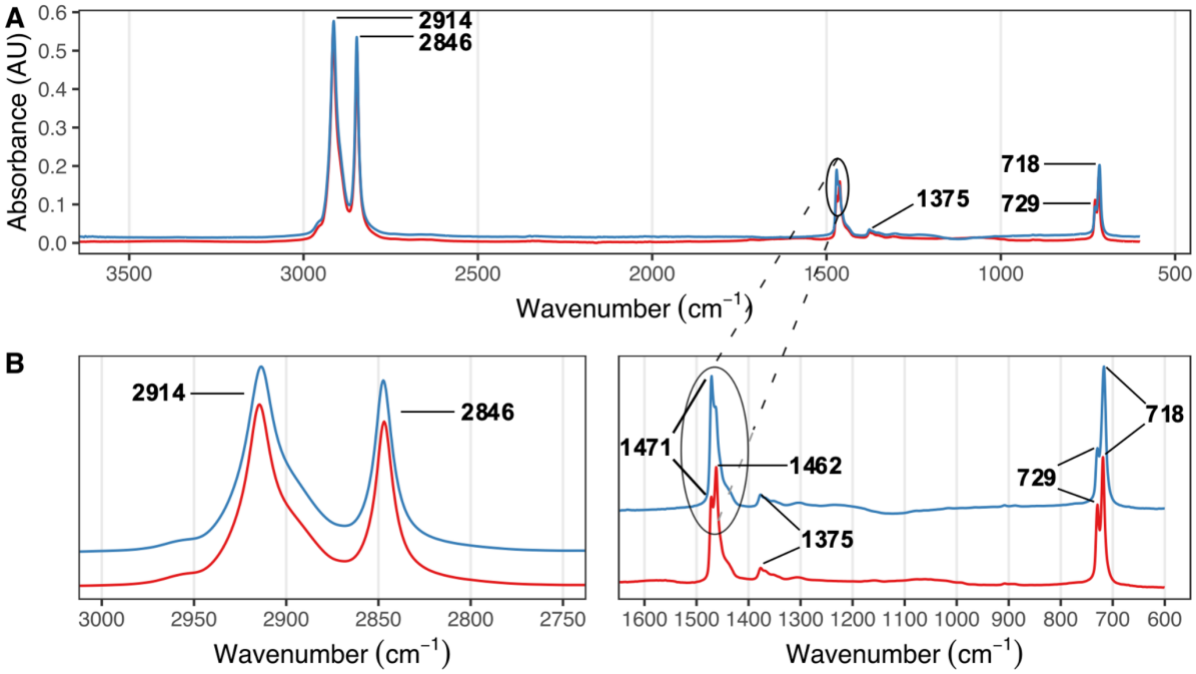

*Figure 23. ATR-FTIR spectra of LDPE TO 1 (red) and 2 (blue). Full spectral range (3500 – 600 cm^{-1}) of both LDPE TOs (**A**). Spectra of region 3000 – 2750 cm^{-1} with peaks at 2914 and 2846 cm^{-1}, and region 1600 – 600 cm^{-1} with peaks at 1471, 1462 (only red), 1375, 729 and 718 cm^{-1}(**B**). The spectra are given an offset of 0.1 Absorbance (AU) to prevent overlap.*

The observed difference between the spectra of LDPE TO 1 and 2 / 3 can be summarized as the difference in vibrational modes (Table 12). The peak at 1471 cm^{-1} comes from vibrational mode CH_2 Scissoring, which can be split into two peaks: 1471 and 1462 cm^{-1}. The former is the case for LDPE TO 2 / 3, and the latter is the case for LDPE TO 1. Split peaks also occur in vibrational mode CH_2 Rocking, which applies to both LDPE TO 1 and TO 2 / 3 with the peaks 729 and 718 cm^{-1}. The observed differences in peak splitting (or the absence of splitting) depend on the physical properties of the material where the proportion of crystallinity is decisive.

Table 12. Overview of ATR-FTIR peaks of the two different LDPE products used in this experiment (i.e., LDPE TO 1 and 2 / 3 derive from two different sources) and their corresponding vibrational mode. The peaks are given in wavenumber cm^{-}.[1]

Vibration	LDPE TO 1 (cm^{-1})	LDPE TO 2 / 3 (cm^{-1})
CH_2 Asymmetric Stretch	2914	2914
CH_2 Symmetric Stretch	2846	2846
CH_2 Scissor	1471	1471
CH_2 Scissor (split peaks in crystalline materials)	1462	No peak
CH_3 Symmetric Bend (umbrella mode)	1375	1375
CH_2 Rocking	729	729
CH_2 Rocking (split peaks in crystalline materials)	718	718

Visualization of potential changes in the LDPE by fungi was done by Principal Component Analysis (PCA). The PCA creates an 2D plot based on correlations among samples and thus similar samples will cluster together. Visualization of potential changes in the LDPE by fungi was done by applying principal component analysis (PCA). PCA results can be used to visualize similarities between samples by creating 2D plot based on the scores. In the score plots similar samples will cluster together. The PCA was conducted on the wavenumbers (cm^{-1}) within the full range and CI-region spectra of the LDPE TOs (Figure 24 & Figure 25). The different observations were labelled by isolates where each isolate is represented by six data points: 30, 60 and 90 days of incubation, with or without glucose. The PCA analysis of the full range spectra resulted in a PC1 of 49 % and a PC2 of 25 %, which combined explain almost 75 % of the observed variation within the spectra (Figure 24 – A & C). The CI-region spectra resulted in a PC1 of 81 % and PC2 of 8 % accounting almost 90 % of the observed variation (Figure 24 – B & D). The lack of clustering indicates no clear correlation or trend for the different isolates.

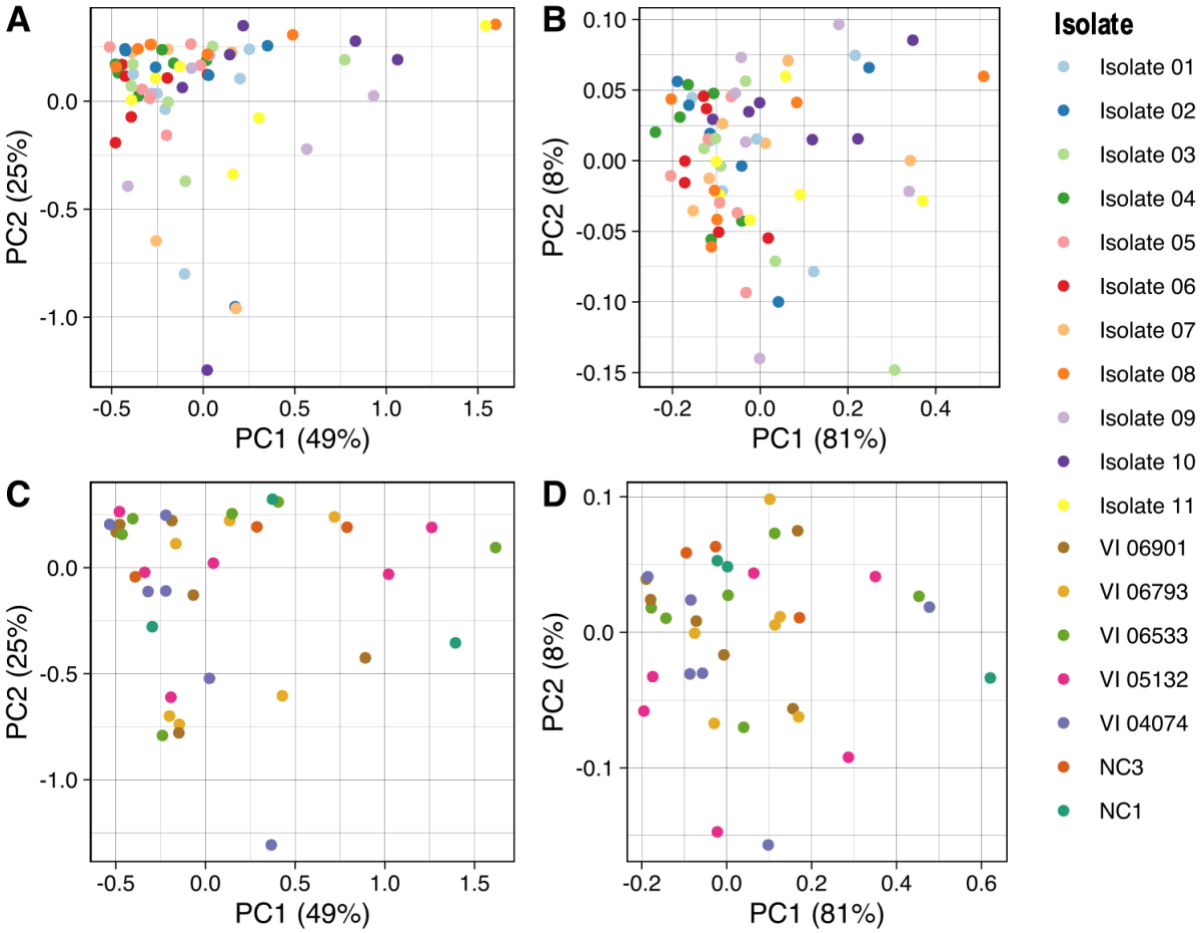

*Figure 24. PCA score plots (PC1 v. PC2) of ATR-FTIR spectra of averaged LDPE TOs grouped by isolate. Spectra from one sample (e.g., Isolate 10 incubated with glucose for 60 days) are manually checked, trimmed, baseline corrected, and triplicates are averaged. Full spectral range 3500 – 600 cm^{-1} (**A** and **C**) and CI-region 1850 – 1420 cm^{-1} (**B** and **D**). The PCA plots are based on the different wavenumbers (cm^{-1}). In **A** and **B**, observations are grouped by isolate (01 – 11), and in **C** and **D**, observations are grouped by reference isolates (VI strain) and negative controls (NC1 and NC3). In each plot, each isolate is represented by six data points from 30, 60 and 90 days of incubation, with or without glucose.*

Here, the PCA results were labelled by incubation interval and the presence / absence of glucose (Figure 25). The PCA grouped by 30, 60 and 90 days of incubation shows some greater variation within the 30 days than the other two (Figure 25 – A & B). The 60 days incubation group presents the tightest clustering. These trends are independent of whether it is full spectrum PCA or PCA based on the CI-region. The importance of the presence of glucose on the observed variation appears to be insignificant for the full range spectrum (Figure 25 – C), but there may be a slight difference between these two groups in the CI-region (Figure 25 – D).

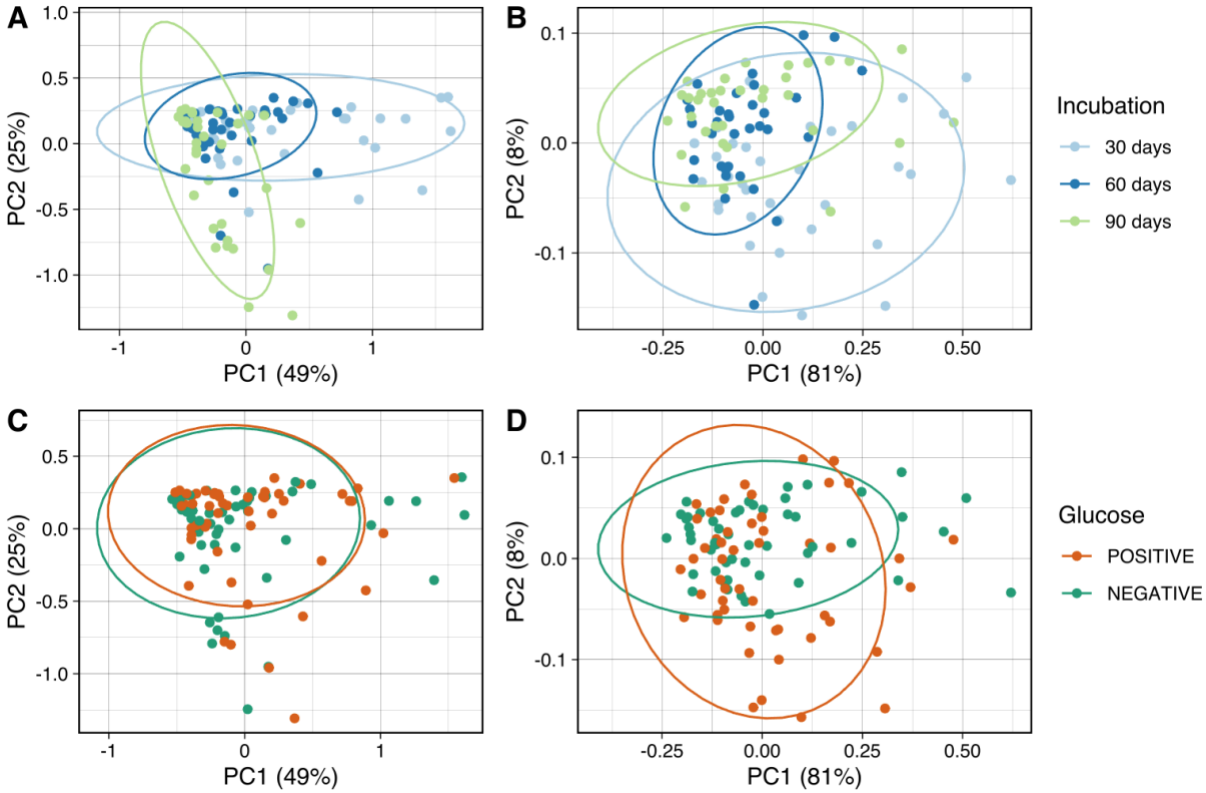

*Figure 25. PCA score plot (PC1 v. PC2) of ATR-FTIR spectra of LDPE TOs grouped by incubation interval or presence / absence of glucose. Spectra from one sample (e.g., Isolate 10 incubated with glucose for 60 days) are manually checked, trimmed, baseline corrected, and triplicates are averaged. Full spectral range 3500 – 600 cm^{-1} (**A** and **C**)) and CI-region 1850 – 1420 cm^{-1} (**B** and **D**). The PCA plots are based on the different wavenumbers (cm^{-1}) and grouped by the incubation time (**A** and **B**) and presence / absence of glucose (**C** and **D**). In any given group 95% of the samples are encircled.*

The respective loadings for the PCs are used to determine what variables cause the greatest impact on the variation. The loading of PC1 and PC2 (of the score plots shown in Figure 24 & Figure 25) indicate that much of the observed variation is due to differences in the absorbance intensity within common peaks and the surrounding frequencies and the qualitative differences in the spectra are minimal (Appendix 6.2.2 Attenuated Total Reflection Fourier Transform Infrared spectroscopy). This corresponds to what has already been observed visually at the spectra and score plots where there are no new prominent peaks.

3.5 Scanning electron microscopy results

Scanning electron microscopy (SEM) analysis was performed to determine if there were any observational changes in topography on the various LDPE TOs that could result from degradation by fungi. Due to the fact that the previously described results were highly ambiguous in the question of degradation, isolates were selected for SEM based on general observations or previous reports. A total of six isolates and three controls were analyzed by SEM. SEM images from two controls (NC1 and NC3) and three isolates (Isolate 01, 06 and VI 05132) incubated at 20 °C for 90 days are presented in Figure 26.

The SEM images of LDPE TOs derived from NC1 showed a relatively smooth and clean surface (Figure 26 – A), with some surface fractures and breaks at higher magnifications (Figure 26 – B & C). The LDPE TOs from NC3 shows the same as NC1, an overall smooth surface (Figure 26 – D) with some surface fractures and breaks at higher magnifications (Figure 26 – E & F). The presented topographically changes in NC1 and NC3 are probably due to mechanical influence, such as handling with tweezers, and not biological factors.

Isolate 01 and 06 were selected based on observed fungal growth on the surface of the LDPE TOs even in the samples without glucose and VI 05132 had some discoloring of the LDPE TOs with the presence of glucose. SEM images of LDPE TOs from Isolate 01 shows fungal growth on the surface (Figure 26 – G) and some roughness of the LDPE TOs surface (Figure 26 – H & I). One can also observe two fungal spores (Figure 26-H S) of Isolate 01. For Isolate 06 cracks and pits in the surface topography of the LDPE TOs can be seen (Figure 26 – J, K & L). Highly probable bacterial contamination (Figure 26 – J C) was observed at the Isolate 06 in the sample without glucose. The overview and closeups of a LDPE TO from isolate VI 05132 shows heavy fungal growth (Figure 26 – M) and some cracks and pits in the surface (Figure 26 – N & O). A fungal spore and hyphae (Figure 26 – N S & H) of VI 05132 can be observed.

The other isolates analyzed by SEM were VI 04074, VI 06901 and Isolate 09 incubated with and without glucose for 90 days. VI 04074 and VI 06901 were chosen for investigation due to high biomass. Isolate 09 was selected at random because it was logistically possible. None of these samples showed any signs of degradation or surface changes due to biological factors. The positive oxidation control was also examined by SEM, but no topographic changes were found.

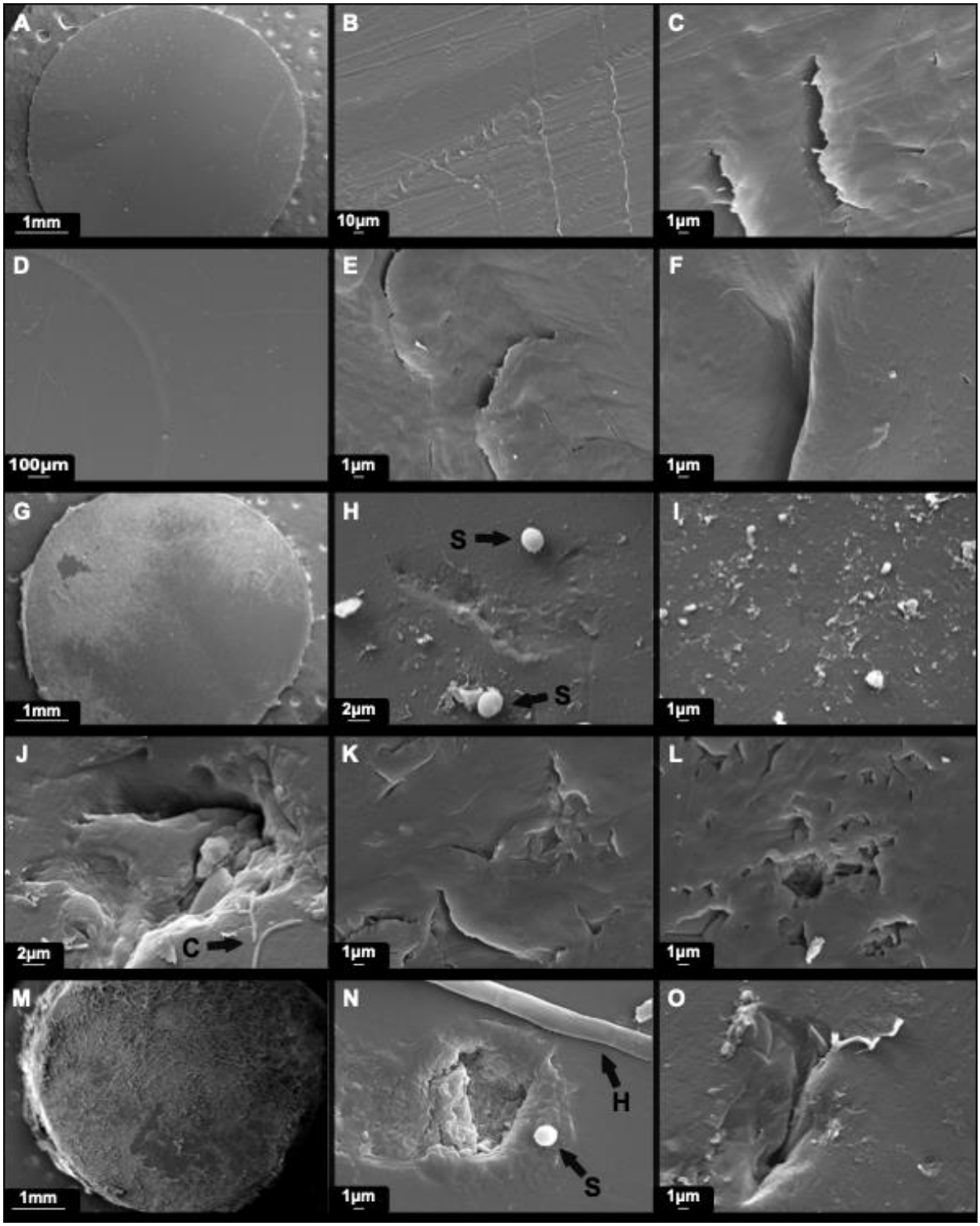

*Figure 26. SEM images of five different samples. The samples were incubated at 20 °C for 90 days. (**A**, **B** and **C**) An overview and closeups of a LDPE TO from negative control without glucose (NC1). (**D**, **E** and **F**) An overview and closeups of a LDPE TO from negative control with glucose (NC3). (**G**, **H** and **I**) An overview and closeups of a LDPE TO from Isolate 01 without glucose (**G** and **H**) and with glucose (**I**). (**J**, **K** and **L**) Closeups of a LDPE TO from Isolate 06 without glucose (**J**) and with glucose (**K** and **L**). (**M**, **N** and **O**) An overview and closeups of a LDPE TO from reference isolate VI 05132 with glucose. Scaling and corresponding scale bar at the bottom left corner. Black arrows indicate S, spore; H, hyphae; C, contaminant.*

4 Discussion

The purpose of this pilot study was to develop new knowledge and build research competence the society and business might need to face the plastic problem through fungal biodegradation. SEM imaging revealed potential evidence of biological degradation in three of the fungal isolates, even if no changes in the test objects were observed by ATR-FTIR or in the freeze-dried biomass or test object weight loss, regardless of presence of glucose, isolate or incubation period. Due to a restricted number of tested isolates and species the results are non-conclusive on fungal capabilities of degrading LDPE. There is a need for improved study design and methodology for further studies.

4.1 Characterization of fungal species

A total of 37 fungal isolates were isolated from soil samples from the different sites. After the selection process, there were 21 isolates left for the second growth rate experiment, incubated at 20 °C for 14 days on ½ PDA. The growth rate test was performed with both the 21 soil isolates and the 5 isolates from *Mykoteket*. Of the total 16 isolates used in the main experiment, the 13 *Trichoderma* spp. covered the entire petri dish (∅ = 9 cm) within 7 days. This was not unexpected as *Trichoderma* is a well-known fast growing soil mold. The species *Aspergillus terreus* (VI 05132), *Aspergillus sydowii* (VI 06533) and *Penicillium chrysogenum* (VI 06901) did not cover the petri dish within 7 days, as was expected since these species have optimal growth conditions at temperatures closer to 30 °C (35). The incubation temperature for the primary screening at 20 °C was based on the reasoning that isolates from Norway's boreal environments have an optimal growth temperature below the standard culture temperature of 25 °C for mesophilic fungi. This hypothesis could have been better investigated with parallel experiments at different temperatures inoculated with the same spore concentrations.

The morphological and molecular characterization identified the 11 soil isolates as species in the genus *Trichoderma*. Molecular identification was done by ITS and *tef1* sequencing. ITS sequences showed highest similarity with the genus *Trichoderma* for all the isolates with an identity > 99 %. Given that the similarity threshold is ≥ 76 % for the query strain to be within the genus *Trichoderma* spp, the genus call was most likely accurate for all the isolates (37).

The results of the species identification can be misleading, as this does not meet the state-of-the-art procedure for *Trichoderma*. Identification of *Trichoderma* at species-level, as with many other fungal species, is quite challenging due to the high number of closely related species. It is an intricate and laborious task that require training and experience within mycology, molecular biology, bioinformatics and state of the art taxonomic literature and procedures. Even with these acquired skills most experts find species identification challenging (37). In 2005 there was proposed an automated DNA Barcoding tool for *Trichoderma* using ITS as sole loci (63). This is no longer the recommended approach for molecular identification of *Trichoderma* species (37). A more manual procedure has been proposed that requires three DNA loci (ITS, *tef1* and *rpd2*) were the obtained sequences needs to be prepared (trimmed) according to the online tool TrichoKey before analysis by BLAST-search and phylogenetic analysis (37). Sequences of ITS and *tef1* obtained in this study did not undergo such a pretreatment, and the ends were just trimmed for higher quality sequences. RNA Polymerase B subunit II (*rpd2*) sequences were not collected at all in this study. It is therefore recommended that the sequences, both ITS and *tef1*, undergo the trimming to retrieve specific sequence fragments. These sequence fragments may then be submitted for sequence similarity search, which will generate more accurate results. In the event of re-identification of the isolates, it is recommended that the same procedure be performed with *rpb2* as with ITS and *tef1*. Phylogenetic analyzes of *tef1* and *rpd2* should also be performed to validate the species identification. The species identification was not conclusive when considering all these factors.

4.2 Scanning Electron Microscopy, weight loss of Test Objects, Attenuated Total Reflection Fourier Transform Infrared and lyophilized biomass

SEM was used to investigate whether there were any surface changes in any of the LDPE TOs. From the small selection of isolates that were selected for screening by SEM, Isolates 01, 06 and VI 05132 were the most interesting. Cracks and pits were evident in the images from Isolate 06 and VI 05132, as they spanned several micrometers. These changes in the topography of the LDPE TOs seemed unsystematic and were deemed to not originate from mechanical stress. It is therefore proposed that these structural surface changes were due to biological factors. This is substantiated by the fact that no similar features were found on the controls (NC1 and NC3). The structural changes found on the controls were characterized as being of a mechanical nature, as these fractures and holes were repeated over larger distances. It is this systematic repetition which characterizes material wear as mechanical in nature. The controls were analyzed with great scrutiny to ensure that no irregular surface fractures could be detected on the controls. Contamination was found in the samples of soil Isolate 06, which was believed to be bacteria. This contamination was only detected by SEM and was never confirmed. Therefore, these results were ambiguous in the question of whether the changes were due to fungi or contamination. In the case of soil Isolate 01 and VI 05132, it is suggested that the findings derive from the fungal degradation.

These were modest SEM results when compared with the findings of other publications. After 90 days of incubation, topographic changes in the 100 μM dimension have been reported, as opposed to 1 - 10 μM observed in this study (29). It should be noted that these studies used higher incubation temperatures during the experiment along with several other factors that make the comparison between the studies difficult.

In this study the total weight of the added LDPE TOs was established on day zero, prior to the start of the experiment. One of each LDPE TO type was randomly selected and weighed after each given incubation period (30, 60 and 90 days). The literature has shown that it might make a difference to the degradation potential if there is an additional highly available carbon source present (64). To investigate this, half the samples were incubated with glucose. The presence of glucose had no significant effect on plastic degradation, given the conditions of

this study (Figure 18). Based on the distribution of observations grouped on the presence of glucose, there were few clusters. Soil Isolate 09 and VI 06793 were seen to have a clustering of the observations for LDPE TO 2, where growth with glucose was somewhat heavier than without. Since the same tendency was not observed with LDPE TO 3 (same origin as TO 2), this suggests that the observed clustering was coincidental and not due to the presence of glucose. Had glucose affected plastic degradation, it could be assumed that this could be observed across LDPE TOs and between the isolates. Due to the lack of significant effect of glucose addition the weight measurements of TOs, samples incubated with or without glucose were combined as a statistical test group to gain statistical strength.

It was assumed that 90 days of incubation would yield a greater effect than 30 or 60 days. While there was a statistically significant difference between the control group and the samples 60 and 90 days of incubation of LDPE TO 1. The difference was greater between the control group and samples incubated for 60 days (p *-value* < 0.01) than the control group and samples incubated for 90 days (p*-value* < 0.05). However, the lower extreme values (observations between 18.00 - 18.25 mg, Figure 19 – A) were equal across all groups, including the control so this statistical significance should be taken with a pinch of skepticism. This significance may not have a real biological effect and was not investigated further at the isolate level. No statistical difference was shown for LDPE TO 2 and LDPE TO 3 and were consequently not investigated further at the isolate level.

To ensure comparable results with other studies, plastic degradation was recorded as relative weight loss. The relative weight loss was calculated as the weight of a test object at the end of incubation relative to the mean weight of the control group. The maximum relative weight loss of LDPE TO 1 was 3.4 % in sample VI 06533 incubated without glucose for 90 days (Figure 20). This weight loss was marginal when compared to other studies that report a relative weight loss of 40 % after 90 days of incubation (29, 30). A weight gain was also observed for several TOs. The greatest variation was seen in the smallest plastic pieces, LDPE TO 2 and 3. Statistically the relative weight loss should have been calculated by the weight of a TO before (day zero) relative to its weight after the incubation period. This would have reduced the observed variation since the initial and final measurement would have been specific to each plastic object. An alternative to this is to measure the total amount of added LDPE at the start, and re-measure the LDPE at the end of incubation. This was the initial method but was not performed due to the size and fragility of the test objects. LDPE TO2 and

3 were especially small and were easily destroyed or lost during handling or not recovered from the mycelium. Any measurements of the end of incubation weight would therefore run the risk of being highly inaccurate and misleading. It was therefore considered the lesser of two evils to calculate the relative weight loss as described in Materials & Methods (2.7).

Another weakness is that the weight was calculated from only one observation per LDPE TO at the given isolate with or without glucose incubated at 30, 60 or 90 days. The fact that only one LDPE TO was measured for each isolate / glucose / incubation period is again due to the large loss of TOs. To standardize the measurements, it was therefore decided that only one from each LDPE TO should be measured.

The LDPE TOs were analyzed by ATR-FTIR to investigate potential oxidation. A positive oxidation control was produced that demonstrated carbonyl containing functional groups in the Carbonyl-Index (CI) region of the spectrum. This peak at 1714 cm^{-1} was relatively small, but with increased oxidation would increase both in intensity and the number of wavenumbers (42). After normalization (baseline correction), all the spectra from the degradation experiment were manually inspected, and none of the TOs showed any sign of carbonyl containing functional groups, as compared to the positive oxidation control.

What the ATR-FTIR spectra did show was a difference between the different types of LDPE TOs. During the analysis for potential oxidation, it was discovered that the two sources of LDPE gave two slightly different spectra indicating slightly different chemical compositions. It was assumed before this observation, that all plastic products marketed as LDPE should generate the same ATR-FTIR spectrum. Consequently, the LDPE TOs were not tested to confirm that the LDPEs had the same chemical makeup as that was beyond the scope of this study. LDPE TO 1 originated from one source (1 mm thick LDPE sheets, Goodfellow) whereas LDPE TO 2 / 3 originated from another (minigrip® LDPE zip-bags, JOKA packaging).

The difference in composition of the LDPEs was unfortunately not detected until after the experiment was completed. The observed difference applies to the two peaks at 1471 and 1462 cm^{-1} which also happen to be the peaks that make up the reference region for the CI-region. While LDPE TO 1 have both peaks, LDPE TO 2 / 3 have only the 1471 cm^{-1} peak. On the other hand, the LDPE TO 2 / 3 peak has a higher intensity than the LDPE TO 1. The

difference in spectra between LDPE TO 1 and 2 / 3 can be explained by the degree of crystallinity in the TOs. In crystalline polyethylene, such as HDPE, the peak at 1471 cm^{-1} was split in to two peaks: 1471 and 1462 cm^{-1} (Figure 23). This is due to long chained alkenes which generates two vibrational modes of CH_2 Scissoring. The same phenomena happen at the 729 / 718 cm^{-1} split with the vibrational mode CH_2 Rocking. The side chains in LDPE force the methylene chains apart, preventing crystallization. Therefore, LDPE does not exhibit this splitting (not as crystalline as HDPE). This indicates that LDPE TO 1 may not be strictly LDPE but something in between LDPE and HDPE as LLDPE (48). When it comes to LDPE TO 2 / 3, these have also split peaks at CH_2 Rocking, which indicates that this plastic was not strictly amorphous either. The impact of these differences in physical properties on the results of this study is not clear, but this result was valuable, as future work on the degradation of any plastic should analyze the chemical composition of the specific plastics investigated.

To see if there were any differences or correlations not readily obvious, the spectra were analyzed by Principal Component Analysis (PCA). Grouping the observations from the PCA of a given isolate may indicate whether there is any trend at the isolate level or if there were any isolates that stands out in particular. It is assumed that the difference in crystallinity has little effect on the PCA, because all triplicates from each isolate / glucose / incubation period consist of an LDPE TO 1, a TO 2 and a TO 3, from which a mean spectrum is then made. Based on this labelling on isolate level, it may indicate that the variation observed was more due to random chance than something systematic as there were no clusters or trends (Figure 24). None of the soil isolates or reference strains from *Mykoteket* stood out significantly. The controls NC1 and NC3 appear to have the same type of scatter relative to the other isolates, which supports the hypothesis of random chance. This trend, or rather the lack of trend, applies to the full spectrum as well as the spectrum that consists only of the CI-region.

When labelling the spectra by incubation time, it may seem that there was a greater spread of the observations at 30 days of incubation than at 60 and 90 days (Figure 25). The spectra of the samples incubated for 60 days had less variation than those incubated for 90 days, which still had less variation than those incubated for 30 days. These trends are evident in the PCA of the whole spectrum and of the CI-region. A possible reason for the difference between the incubation times may be the different washing procedures after each given incubation. The spectra of the samples incubated for 30 days which were the samples washed most gently, and

these may thus be contaminated with residues from MSM and the mycelium to a greater extent than TOs incubated for 60 and 90 days.

When labelling observations (spectra) by the presence of glucose, it may seem that there was no difference in PCA of the full spectrum. PCA of the CI-region may at first glance indicate that there was a greater variation in samples with glucose compared to those without. However, as Principal Component 1 (PC1) makes up 81 % of the observed variation this interpretation may need reconsidering. The greatest observable spread within a group, is shown in the PCA plot (Figure 25 – D) to be within the group of samples with glucose compared to those without. This spread, however, was explained by PC2 which only accounts for 8% of the variation. While the variation within the group within glucose is mostly explained by PC1 as seen in the shape of the encircled 95 % of observations. As a consequence, it is difficult to draw any informative conclusions from the PCA analysis at this stage. The loading scores indicate that the variation in the PCA was due to the difference in the intensity of the prominent peaks rather than any changes in the CI-region. With a positive oxidation control in the PCA this could have given an indication of how oxidation could have affected the analysis.

Measuring dry biomass was used to indirectly see if there was any degradation of LDPE TOs. There was no clear trend individually for the isolates between the time series regardless of whether glucose was present or not. There is, however, a clear trend between with and without glucose on a general level. Growth with glucose has clearly resulted in increased biomass. This was not unexpected as glucose is a carbohydrate that most microorganisms can metabolize. It should also be noted that 100 mL of MSM with 2 % w / v glucose only corresponds to a carbon source of 800 mg carbon. Hypothetically, if the carbon to biomass increase ratio was 1:1 and 1 mg carbon yields a 1 mg increase in biomass, this would only result in an average of 67 mg of increased biomass with LDPE as a carbon source. The real ratio has not been calculated in this study. Degradation of LDPE by fungi using it as a carbon source could be detected, by recording acquired biomass in incubations where no other carbon source is available. Measuring this increase in biomass due to LDPE in incubations with glucose is currently not feasible. This is because the biomass increase with glucose as a carbon source would be exponentially higher than that of LDPE as a carbon source, simply due to glucose being easier to metabolize. What caused the statistical outliers is not clear, but they were probably not due to biological factors.

The sizes of the TOs 2 and 3 were problematic. As previously mentioned, they were very small, fragile, and tricky to handle due to both their size and static electricity making them cling to surfaces and tools. There was therefore no guarantee that all the pieces of plastic, especially the smallest ones, were removed from the mycelium. A possible alternative solution could be to start with a given number of plastic pieces, which then can be compared with the number that was retrieved at the end.

Growth was measured in all controls at one or more time points during the incubation intervals. A lyophilized biomass of 10.51 mg for NC1 and 15.06 mg for NC2 was measured by incubation without glucose for 90 days. This was significant compared to the average for 90 days incubation without glucose, which was 3.19 mg. No growth was expected in any of these controls. For NC1, there should not have been any growth as this contains only MSM and LDPE TOs, and no fungal inoculum. This indicates contamination of the sample or an issue with the weight measurement. NC2 should not have had growth either, as this was inoculated with the control species *T. harzianum* but did not contain any carbon source, neither glucose nor LDPE. Growth was also observed in the two controls with glucose, NC3 and PC1.

NC3 should in principle have no growth, as this should only contain MSM, LDPE TOs and glucose. There was a slight increase in NC3 at 60 and 90 days, 62.43 and 72.77 mg, respectively. This was slightly below the average and the median for the given incubation period, but did still clearly indicate growth. This indicates that the sterile technique was not sufficient and resulted in contaminated controls. Another source of contamination may be that the aluminum lid was only loosely attached to provide aerobic conditions. A filter of sterile cotton in the bottleneck could have kept potential airborne spores out and counteracted this risk. The presumption that the source of contamination was airborne may be supported by the fact that no growth was found during NC3 on 30-day incubation. Future trials should consider whether a filter should be used in the bottleneck to prevent airborne contamination. Growth in positive control 1 (PC1) was measured at all incubation intervals. This is highly desirable as it suggests that MSM with glucose does not inhibit the growth of fungi since PC1 was inoculated with *T. harzianum*. It should be mentioned that all the measurements were somewhat lower than the average and the median, with no sufficient explanation for this. It was highly unfortunate that there was growth in the negative controls (NC1, NC2 and NC3),

but it may be assumed that this has no real impact on the results from this experiment. Nevertheless, this should be considered and investigated in similar subsequent experiments.

The failure of the *Mykoteket* reference strains in demonstrating greater degradation of the LDPE test objects was unexpected, as these, with exception of *T. trixiae,* are already associated with degradation of LDPE (28-31).However, there were several factors that when combined may have reduced biodegradation potential. The incubation temperature for the experiment was 20 °C, which was lower than the reference studies, which had incubation temperatures of 25 °C or not specified at all (29-31, 64). The great diversity in PE plastic materials may also have contributed, as the LDPE TOs used in this study may be different from those in other studies. The LDPE TOs may contain various substances that might reduce the oxidation potential and thus the degradation. Lastly, species from different geographical locations may have somewhat different expressions of some traits, as micro differences in biotic and abiotic factors of the different environments will result in adaptation and give rise to intraspecific variation (65).

There is no clear conclusion as to the LDPE degrading potential of any of the isolates based on the results from SEM, ATR-FTIR, weight loss on LDPE TOs and freeze-dried biomass as a whole. The SEM results may indicate a biodegradation potential in some of the isolates, but this was not supported by the results of the other analysis methods.

While isolates where characterized from different environments associated with plastic handling in Norway, the results are inconclusive as to whether they have any LDPE degrading potential. Whether it was due to weaknesses in the study design, or confounding factors such as the chemical composition of the LDPE used, the reasons for why the results are inconclusive may be many. What this study does offer is a starting point for further research into plastic degrading fungi isolated from Norwegian environments. May this study inform those intrepid few who brave the utter chaos of plastic pollution and the enigmatic jungles that is mycology.

4.3 Future research

There are several aspects that later research should improve and explore when investigating the degradation of PE plastics. One of these is to develop and optimize a method for conducting experiments to test the biodegradation potential of fungi. It should be a priority to define a practical and appropriate size of the plastic pieces to be used. The test objects should be so large that they can either be marked or recognized before and after the end of the experiment, which can give reliable results in terms of weight loss and potentially be used for testing tensile strength. As shown in this study, the uncertainty in measurements of smaller test objects is too great to be conclusive.

Plastic is a hodgepodge of various chemical substances where even the production method will determine critical properties. This also applies within the family of polyethylene plastic. The plastic used in further experiments should be clearly defined, everything from production method, technical details to additives. This is one of the sources of error in the current study, where there is no full disclosure regarding potential fillers, UV-absorbers or antioxidants. It would be appropriate to test fungal isolates that have demonstrated degradation potential on a transparent plastic product and then test it on common PE articles such as round bale wrapping, bread bags etc.

Based on this study ATR-FTIR and SEM are appropriate analytical methods for determining LDPE degradation and is recommended for further research. ATR-FTIR has the advantages of virtually no sample preparation, the analysis itself is fast and the data processing can be automated to a certain extent. This makes ATR-FTIR highly economical and time efficient (66). Another advantage is that ATR-FTIR has been proposed as a standard for analysis of oxidation in accelerated aging (thermo- and photooxidation) of plastics (42). Standardizing methods is important for comparable results across studies. A disadvantage of ATR-FTIR is that the actual analysis area is limited to the size of the crystal in the ATR unit which is only a few millimeters in diameter. As indicated in the SEM images, potential initial biological oxidation and degradation will be highly localized, which makes missing an oxidized area a risk when performing ATR-FTIR analysis.

SEM is the exact opposite of ATR-FTIR, where SEM has a substantial sample preparation, the analysis takes 30 - 60 minutes per sample and has virtually no possibility for automation. Access to a scanning electron microscope is obviously also a requirement, which should not be taken for granted as they are quite expensive. In other words, SEM is an expensive and time-consuming analysis method, compared to ATR-FTIR. On the other hand, it is more thorough than ATR-FTIR where it is possible to observe micrometer-sized surface changes to the sample.

If PE degrading fungal isolates are found, it will be highly appropriate to study the mechanisms behind the degradation. There is a great need for this type of research, as there is very little characterization of biochemical, enzymatic and mechanical mechanisms associated with biodegradation of PE (26). Two mechanisms unique to filamentous fungi that are of potential interest are the hydrophobins and appressorium. Hydrophobins are small secreted proteins which are related to processes that, among other things, involve attachment to hydrophobic surfaces (67). Another interesting property some fungi have is the formation of specialized cells called the appressorium. Appressorium are specialized hyphae that can penetrate plant cells and other synthetic materials due to turgor pressure. This pressure is caused by osmotic flow of water over a semipermeable membrane that can reach extreme pressures (68).

The world is swimming in plastic waste, with no apparent single solution to the problem. It is conceivable that research on plastic degrading fungi may provide insight into several ways to deal with the plastic problem. The obvious thing is where plastic degrading fungi can be used directly to break down plastic waste regardless of whether it is via a waste management system or not. If it is through a waste management system, it will hypothetically be able to contribute to material recycling where the plastic material is degraded to its constituents. Outside of organized collection, private individuals may be able to compost household plastic waste, or perhaps the fungus inoculum can be spread in exposed places. Regardless of the area of use, it is critical that the plastic is not only broken down into micro- and nanoplastics and then contaminates the environment. For it to be a sustainable and considerate solution, the fungus must either degrade the plastic into harmless molecules totally assimilate its molecular constituents.

Further research can contribute to other sustainable solutions such as the development of biodegradable plastic types or novel polymer materials. Insight into how enzyme complexes catalyze the reactions, and which molecular bonds are broken is vital for future research.

5 References

1. Lislevand T. Plasthvalen. snl.no: Store norske leksikon; 2017 [updated 05.01.2021; cited 14.05.2022]. Available from: https://snl.no/plasthvalen.

2. Vianello A, Jensen RL, Liu L, Vollertsen J. Simulating human exposure to indoor airborne microplastics using a Breathing Thermal Manikin. Scientific Reports. 2019;9(1):8670.

3. Leslie HA, van Velzen MJM, Brandsma SH, Vethaak AD, Garcia-Vallejo JJ, Lamoree MH. Discovery and quantification of plastic particle pollution in human blood. Environment International. 2022;163:107199.

4. Geyer R. A Brief History of Plastics. In: Streit-Bianchi M, Cimadevila M, Trettnak W, editors. Mare Plasticum - The Plastic Sea: Combatting Plastic Pollution Through Science and Art. Cham: Springer International Publishing; 2020. p. 31-47.

5. Elhacham E, Ben-Uri L, Grozovski J, Bar-On YM, Milo R. Global human-made mass exceeds all living biomass. Nature. 2020;588(7838):442-4.

6. Borrelle SB, Ringma J, Law KL, Monnahan CC, Lebreton L, McGivern A, et al. Predicted growth in plastic waste exceeds efforts to mitigate plastic pollution. Science. 2020;369(6510):1515-8.

7. MacLeod M, Arp HPH, Tekman MB, Jahnke A. The global threat from plastic pollution. Science. 2021;373(6550):61-5.

8. Persson L, Carney Almroth BM, Collins CD, Cornell S, de Wit CA, Diamond ML, et al. Outside the Safe Operating Space of the Planetary Boundary for Novel Entities. Environmental Science & Technology. 2022;56(3):1510-21.

9. Ore S, Stori A. Plast snl.no: Store norske leksikon; 2021 [updated 31.08.2021; cited 04.05.2022]. Available from: https://snl.no/plast.

10. Merriam-Webster. Plastic: Merriam-Webster.com dictionary; (n.d.) [cited 13.05.2022]. Available from: https://www.merriam-webster.com/dictionary/plastic.

11. Andrady AL, Neal MA. Applications and societal benefits of plastics. Philos Trans R Soc Lond B Biol Sci. 2009;364(1526):1977-84.

12. ASTM International. Standard Practice for Coding Plastic Manufactured Articles for Resin Identification (ASTM D7611/D7611M-21) astm.org: ASTM International; 2021 [updated 04.01.2022; cited 06.03.2022]. Available from: https://www.astm.org/d7611_d7611m-21.html.

13. Okamura T-a. Polyethylene (PE; Low Density and High Density). In: Kobayashi S, Müllen K, editors. Encyclopedia of Polymeric Nanomaterials. Berlin, Heidelberg: Springer Berlin Heidelberg; 2015. p. 1826-9.

14. Merriam-Webster. Packaging: Merriam-Webster.com Dictionary; (n.d.) [updated 21.05.2022; cited 23.05.2022]. Available from: https://www.merriam-webster.com/dictionary/packaging.

15. Grønt Punkt Norge. Plastretur planlegger for norsk sorteringsanlegg: grontpunkt.no; 2021 [cited 14.04.2022].

16. Norsirk. Produsentansvarsselskaper og omdømme norsirk.no: Norsirk; 2017 [updated 02/07/2017. Available from: https://norsirk.no/blog/2017/07/02/produsentansvarsselskaper-og-omdomme/.

17. Grønn Punkt Norge. Fakta og tall - Tall for 2021 rapportert til Miljødirektoratet i april 2022 grontpunkt.no: Grønn Punkt Norge; 2022 [cited 20.05.2022]. Available from: https://www.grontpunkt.no/om-oss/fakta-og-tall/.

18. Thompson RC, Moore CJ, vom Saal FS, Swan SH. Plastics, the environment and human health: current consensus and future trends. Philos Trans R Soc Lond B Biol Sci. 2009;364(1526):2153-66.

19. European Commission. Waste Framework Directive ec.europa.eu: European Union; 2020 [cited 19.05.2022]. Available from: https://ec.europa.eu/environment/topics/waste-and-recycling/waste-framework-directive_en.

20. Milios L, Holm Christensen L, McKinnon D, Christensen C, Rasch MK, Hallstrøm Eriksen M. Plastic recycling in the Nordics: A value chain market analysis. Waste Management. 2018;76:180-9.

21. Bisinella V, Nedenskov J, Riber C, Hulgaard T, Christensen TH. Environmental assessment of amending the Amager Bakke incineration plant in Copenhagen with carbon capture and storage. Waste Manag Res. 2022;40(1):79-95.

22. Hopewell J, Dvorak R, Kosior E. Plastics recycling: challenges and opportunities. Philos Trans R Soc Lond B Biol Sci. 2009;364(1526):2115-26.

23. Store norske leksikon. Plast snl.no: Store norske leksikon; 2009 [updated 31.08.2021; cited 19.05.2022]. Available from: https://snl.no/plast.

24. Voříšková J, Baldrian P. Fungal community on decomposing leaf litter undergoes rapid successional changes. The ISME Journal. 2013;7(3):477-86.

25. Yoshida S, Hiraga K, Takehana T, Taniguchi I, Yamaji H, Maeda Y, et al. A bacterium that degrades and assimilates poly(ethylene terephthalate). Science. 2016;351(6278):1196-9.

26. Danso D, Chow J, Streit WR, Drake HL. Plastics: Environmental and Biotechnological Perspectives on Microbial Degradation. Applied and Environmental Microbiology. 2019;85(19):e01095-19.

27. Singh Jadaun J, Bansal S, Sonthalia A, Rai AK, Singh SP. Biodegradation of plastics for sustainable environment. Bioresource Technology. 2022;347:126697.

28. Srikanth M, Sandeep TSRS, Sucharitha K, Godi S. Biodegradation of plastic polymers by fungi: a brief review. Bioresources and Bioprocessing. 2022;9(1):42.

29. Ojha N, Pradhan N, Singh S, Barla A, Shrivastava A, Khatua P, et al. Evaluation of HDPE and LDPE degradation by fungus, implemented by statistical optimization. Scientific Reports. 2017;7(1):39515.

30. Sangale MK, Shahnawaz M, Ade AB. Potential of fungi isolated from the dumping sites mangrove rhizosphere soil to degrade polythene. Scientific Reports. 2019;9(1):5390.

31. Sowmya HV, Ramalingappa, Krishnappa M, Thippeswamy B. Degradation of polyethylene by Trichoderma harzianum—SEM, FTIR, and NMR analyses. Environmental Monitoring and Assessment. 2014;186(10):6577-86.

32. Kumar Sen S, Raut S. Microbial degradation of low density polyethylene (LDPE): A review. Journal of Environmental Chemical Engineering. 2015;3(1):462-73.

33. Gulden G, Eckblad F-E. Sopp: Store norske leksikon; 2021 [updated 16.12.2021; cited 19.05.2022]. Available from: https://snl.no/sopp.

34. Watkinson S, Boddy L, Money N. The Fungi. 3 ed. Cambridge, US: Academic Press; 2015.

35. Samson RA, Houbraken J, Thrane U, Frisvad JC, Andersen B. Food and Indoor Fungi - Second Edition. Crous PW, Samson RA, editors. Utrecht: Westerdijk Fungal Biodiversity Institute; 2019.

36. Gohil N, Panchasara H, Patel S, Singh V. Molecular Biology Techniques for the Identification and Genotyping of Microorganisms. In: Tripathi V, Kumar P, Tripathi P, Kishore A, editors. Microbial Genomics in Sustainable Agroecosystems: Volume 1. Singapore: Springer Singapore; 2019. p. 203-26.

37. Cai F, Druzhinina IS. In honor of John Bissett: authoritative guidelines on molecular identification of Trichoderma. Fungal Diversity. 2021;107(1):1-69.

38. Wilson K, Walker J. Principles and techniques of biochemistry and molecular biology. 8 ed: Cambridge university press; 2010.

39. Haugen MN, Sonnenberg CB. DNA-sekvensering: Store Norske Leksikon; 2021 [updated 21.07.2021; cited 20.05.2022]. Available from: https://snl.no/DNA-sekvensering.

40. Guttman A, Hajba L. Chapter one - Introduction. In: Guttman A, Hajba L, editors. Capillary Gel Electrophoresis. Boston: Elsevier; 2022. p. 1-20.

41. Durney BC, Crihfield CL, Holland LA. Capillary electrophoresis applied to DNA: determining and harnessing sequence and structure to advance bioanalyses (2009-2014). Analytical and bioanalytical chemistry. 2015;407(23):6923-38.

42. Almond J, Sugumaar P, Wenzel MN, Hill G, Wallis C. Determination of the carbonyl index of polyethylene and polypropylene using specified area under band methodology with ATR-FTIR spectroscopy. e-Polymers. 2020;20(1):369-81.

43. Merriam-Webster. Wave number: Merriam-Webster.com dictionary; (n.d.) [cited 14.06.2022]. Available from: https://www.merriam-webster.com/dictionary/wave%20number.

44. Ozaki Y, Baranska M, Lednev IK, Wood BR. Preface. In: Ozaki Y, Baranska M, Lednev IK, Wood BR, editors. Vibrational Spectroscopy in Protein Research: Academic Press; 2020. p. xxi-xxii.

45. Fellgett PB. On the Ultimate Sensitivity and Practical Performance of Radiation Detectors. J Opt Soc Am. 1949;39(11):970-6.

46. Griffiths PR, Haseth JAD. Fourier Transform Infrared Spectrometry. 2 ed. Winefordner JD, editor: Wiley; 2007.

47. Ausili A, Sánchez M, Gómez-Fernández JC. Attenuated total reflectance infrared spectroscopy: A powerful method for the simultaneous study of structure and spatial orientation of lipids and membrane proteins. Biomedical Spectroscopy and Imaging. 2015;4:159-70.

48. Smith B. The Infrared Spectra of Polymers II: Polyethylene. Spectroscopy. 2021;36(9):24–9.

49. Fjellvåg H. Elektronmikroskop: Store norske leksikon; 2021 [updated 06.11.2021; cited 10.05.2022]. Available from: https://snl.no/elektronmikroskop.

50. JEOL. Scanning Electron Microscope A To Z - Basic Knowledge For Using The SEM jeol.co.jp: JEOL; (n.d.) [cited 08.06.2022]. Available from: https://www.jeol.co.jp/en/applications/pdf/sm/sem_atoz_all.pdf.

51. Joy DC, Bradbury S, Ford BJ. Scanning Electron Microscope: Encyclopedia Britannica; 2019 [cited 11.06.2022]. Available from: https://www.britannica.com/technology/scanning-electron-microscope.

52. Goldstein JI, Newbury DE, Echlin P, Joy DC, Fiori C, Lifshin E. Scanning Electron Microscopy and X-Ray Microanalysis - A Text for Biologists, Materials Scientists, and Geologists. 1 ed. New York, US: Springer New York.

53. Hurt R. Electron emission mechanisms: Wikimedia Commons; 2016 [updated 22.04.2022; cited 22.05.2022]. Available from: https://en.wikipedia.org/wiki/File:Electron_emission_mechanisms.svg.

54. Gregoire JM, Lobovsky MB, Heinz MF, DiSalvo FJ, van Dover RB. Resputtering phenomena and determination of composition in codeposited films. Physical Review B. 2007;76(19):195437.

55. Klima- og miljødepartementet. Endring av emballasjedirektivet (del av pakke sirkulær økonomi) regjeringen.no: Norges Regjeringen; 2014 [updated 12.05.2022; cited 22.05.2022]. Available from: https://www.regjeringen.no/no/sub/eos-notatbasen/notatene/2014/okt/endring-av-emballasjedirektivet-del-av-pakke-sirkular-okonomi/id2502199/.

56. European Commission. Packaging waste - EU rules on packaging and packaging waste, including design and waste management. ec.europa.eu: European Union; 2018 [cited 19.05.2022]. Available from: https://ec.europa.eu/environment/topics/waste-and-recycling/packaging-waste_en.

57. United Nations. Take Action for the Sustainable Development Goals un.org: United Nations; 2022 [cited 14.05.2022]. Available from: https://www.un.org/sustainabledevelopment/sustainable-development-goals/.

58. Dhillion SS, Svarstad H, Cathrine A, Hans Chr B. Bioprospecting: Effects on Environment and Development. Ambio. 2002;31(6):491-3.

59. White TJ, Bruns T, Lee S, Taylor JW. Amplification and direct sequencing of fungal ribosomal RNA genes for phylogenetics. Innis MA, Gelfand DH, Sninsky JJ, White TJ, editors. New York, N.Y: Academic Press; 1990.

60. O'Donnell K, Kistler HC, Cigelnik E, Ploetz RC. Multiple evolutionary origins of the fungus causing Panama disease of banana: Concordant evidence from nuclear and

mitochondrial gene genealogies. Proceedings of the National Academy of Sciences. 1998;95(5):2044-9.

61. Carbone I, Kohn LM. A Method for Designing Primer Sets for Speciation Studies in Filamentous Ascomycetes. Mycologia. 1999;91(3):553-6.

62. Altschul SF, Gish W, Miller W, Myers EW, Lipman DJ. Basic local alignment search tool. J Mol Biol. 1990;215(3):403-10.

63. Druzhinina I, Kubicek CP. Species concepts and biodiversity in Trichoderma and Hypocrea: from aggregate species to species clusters? J Zhejiang Univ Sci B. 2005;6(2):100-12.

64. Khan S, Nadir S, Shah ZU, Shah AA, Karunarathna SC, Xu J, et al. Biodegradation of polyester polyurethane by Aspergillus tubingensis. Environmental Pollution. 2017;225:469-80.

65. Van Rossum T, Ferretti P, Maistrenko OM, Bork P. Diversity within species: interpreting strains in microbiomes. Nat Rev Microbiol. 2020;18(9):491-506.

66. Guiliano M, Asia L, Onoratini G, Mille G. Applications of diamond crystal ATR FTIR spectroscopy to the characterization of ambers. Spectrochimica Acta Part A: Molecular and Biomolecular Spectroscopy. 2007;67(5):1407-11.

67. Chaves AFA, Simões LC, Paterson R, Simões M, Lima N. Chapter 5 - The role of filamentous fungi in drinking water biofilm formation. In: Simoes M, Borges A, Chaves Simoes L, editors. Recent Trends in Biofilm Science and Technology: Academic Press; 2020. p. 101-25.

68. Howard RJ, Ferrari MA, Roach DH, Money NP. Penetration of hard substrates by a fungus employing enormous turgor pressures. Proceedings of the National Academy of Sciences of the United States of America. 1991;88(24):11281-4.

6 Appendix

6.1 Culture media

Culture media and SEM fixative liquid used for this thesis is given below.

Potato Dextrose Agar (PDA)	Difco
Potato dextrose agar	39 g
$ZnSO_4 \cdot 7H_2O$	0.01 g
$CuSO_4 \cdot 5H_2O$	0.005 g
Distilled water	1000 mL

Mix well and autoclave at 121 °C for 15 min.

pH = 5.6 ± 0.2

1/2 PDA	Difco - Merck
Potato dextrose agar	19.5 g
Agar powder	7.5 g
$ZnSO_4 \cdot 7H_2O$	0.01 g
$CuSO_4 \cdot 5H_2O$	0.005 g
Distilled water	1000 mL

Mix well and autoclave at 121 °C for 15 min.

pH = 5.6 ± 0.2

Malt Extract Agar (MEA)	Oxoid (CM0059)
Potato dextrose agar	50 g
$ZnSO_4 \cdot 7H_2O$	0.01 g
$CuSO_4 \cdot 5H_2O$	0.005 g
Distilled water	1000 mL

Mix well and autoclave at 115 °C for 10 min.

pH = 5.4 ± 0.2

Dichloran 18 % Glycerol agar (DG18)	Oxoid
Dichloran-Glycerol-agar-base	31.5 g
Glycerol (anhydrous)	220 g
$ZnSO_4 \cdot 7H_2O$	0.01 g
$CuSO_4 \cdot 5H_2O$	0.005 g
Chloramphenicol	0.05 g
Distilled water	1000 mL

Mix well and autoclave at 121 ° C for 15 min.

Add 0.05 g chlortetracycline after autoclaving.

pH = 5.6 ± 0.2

Reference: Hocking and Pitt (1980)

Mineral Salt Media (MSM)	Merck
Potassium dihydrogen orthophosphate (KH_2PO_4)	0.7 g
Dipotassium monohydrogen orthophosphate (K_2HPO_4)	0.7 g
Magnesium sulfate ($MgSO_4 \cdot 7H_2O$)	0.7 g
Ammonium nitrate (NH_4NO3)	1.0 g
Sodium chloride (NaCl)	0.005 g
Ferrous sulfate ($FeSO_4 \cdot 7H_2O$)	0.002 g
Zinc sulfate ($ZnSO_4 \cdot 7H_2O$)	0.002 g
Manganous sulfate ($MnSO_4 \cdot H_2O$)	0.001 g
Distilled water	1000 mL

Mix well and autoclave at 121 °C for 15 min.

Add 10 g of glucose if 1 % w / v is required.

pH = 6.2 ± 0.2

Reference: ASTM G21-15(2021)

100 mL SEM sample fixation liquid	NA

4 % Paraformaldehyde	50 mL
25 % Glutaraldehyde	5 mL
Buffer *	25 mL
Distilled water	20 mL

Mix well and autoclave at 151 grader C for 10 min.

* MSM (or 0.4 M PIPES) or the appropriate buffer

6.2 Supplementary figures

6.2.1 Weight loss of Low-Density Polyethylene Test Objects

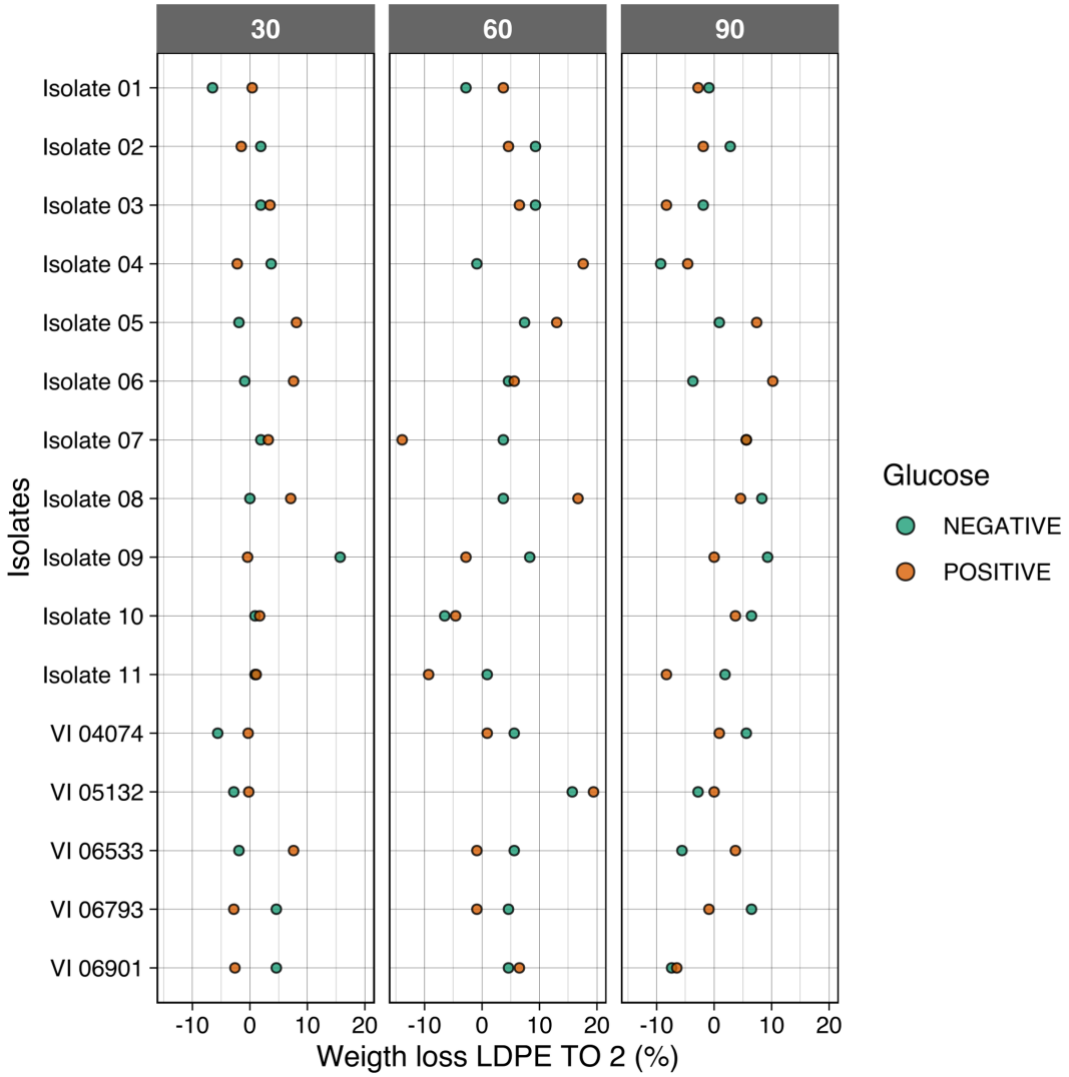

Figure 27. Weight loss in percentage for LDPE TO 2(n = 6 per isolate) through the three incubation periods 30, 60 and 90 days with (positive) or without (negative) glucose.

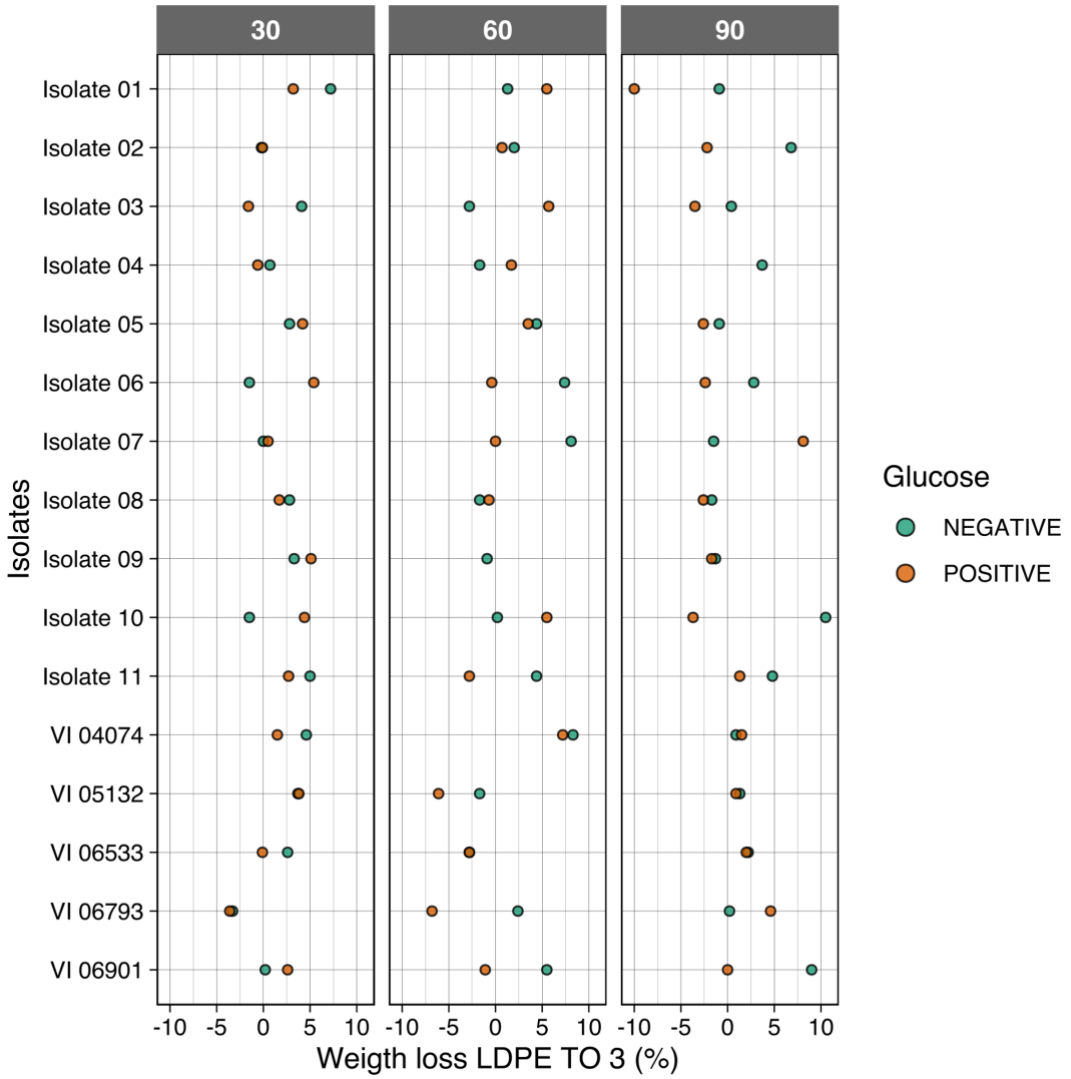

Figure 28. Weight loss in percentage for LDPE TO 3 (n = 6 per isolate) through the three incubation periods 30, 60 and 90 days with (positive) or without (negative) glucose.

6.2.2 Attenuated Total Reflection Fourier Transform Infrared spectroscopy

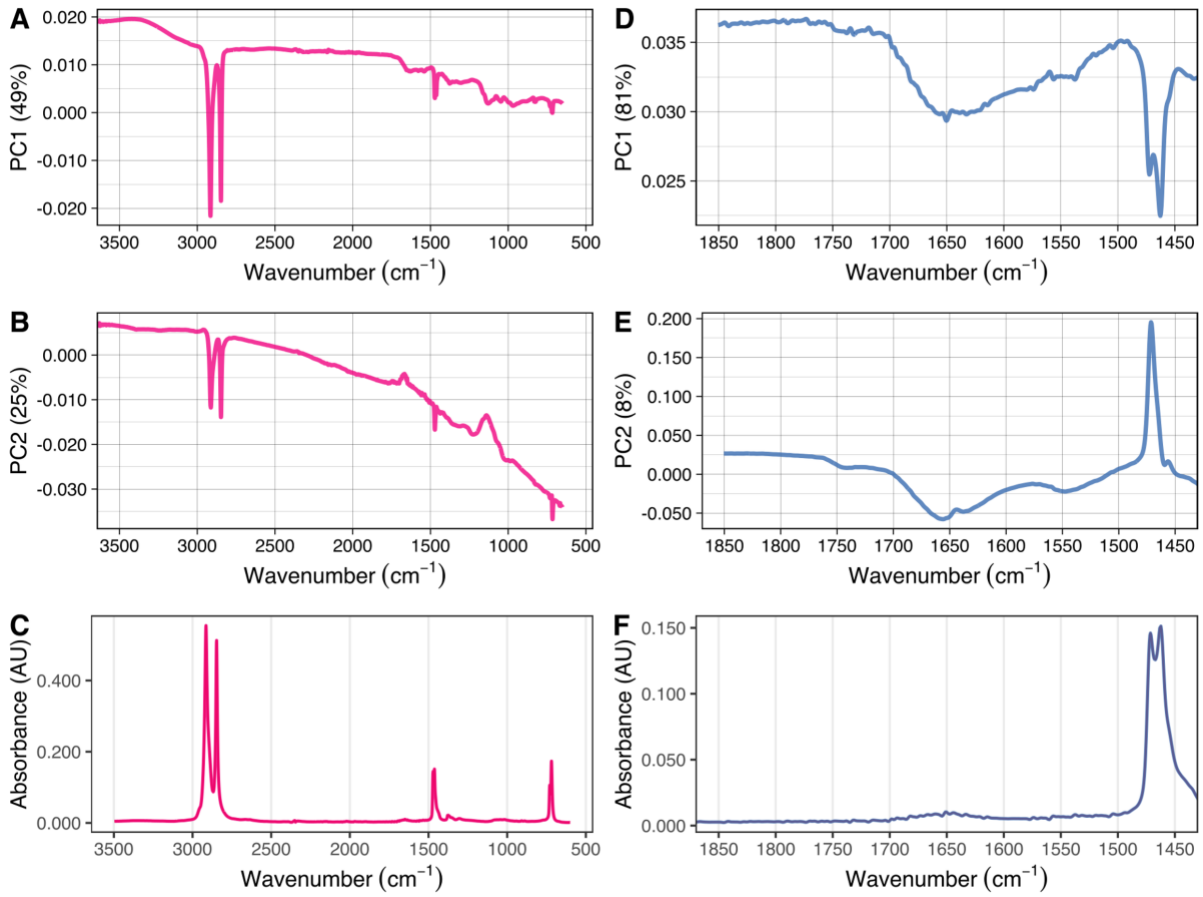

*Figure 29. Loadings plot derived from the PCA with corresponding spectra. Full spectral range (3500 – 600 cm^{-1}) with the respective peaks; 2914, 2846, 1375, 729 and 718 cm^{-1}(**C**) and loadings plot of PC1 (**A**) and PC2 (**B**) from the PCA of full spectral range. The Spectra of Carbonyl index (CI) region (1850 – 1650 cm^{-1}) and reference region (1500 – 1420 cm^{-1}) with the peaks 1471 and 1462 cm^{-1}(**B**) and loadings plot of PC1 (**D**) and PC2 (**E**) from the PCA of CI- region and associated reference region.*

Norges miljø- og biovitenskapelige universitet
Noregs miljø- og biovitskapelege universitet
Norwegian University of Life Sciences

Postboks 5003
NO-1432 Ås
Norway